Monsoon–like climate during the Bajocian
Clay mineralogical and geochemical study on a limestone/marl alternation (Komló Calcareous Marl Formation, Mecsek Mountains, Southern Hungary)

Béla RAUCSIK[1], Attila DEMÉNY[2], Ildikó BORBÉLY–KISS[3], Gyula SZABÓ[3]

[1]University of Veszprém, Dep. of Earth and Environmental Sciences, H–8201 Veszprém, P.O.Box 158.
E-mail: raucsik@almos.vein.hu
[2]Geochemical Research Laboratory of the Hungarian Academy of Sciences, H–1112 Budapest, Budaörsi út 45.
E-mail: demeny@sparc.core.hu
[3]Institute of Nuclear Research of the Hungarian Academy of Sciences, H–4001 Debrecen, P.O.Box 51
E-mail: szgy@cseles.atomki.hu

(With 11 figures and 5 tables)

Jurassic formations are cropped out in the eastern part of the Mecsek Mountains in a relatively extended area. The Aalenian–Bajocian interval is characterised by bioturbated marls and clayey limestones (Fleckenmergel, Allgäu facies) named as Komló Calcareous Marl Formation. The most obvious feature of this formation is rhythmic alternation of carbonate–rich and carbonate–poor semicouplets. Our work deals with characterization of changes of palaeoenvironmental conditions of this sequence using an approach involving study of changes in clay mineral assemblages, determination of stable isotopic composition, and enrichment or impoverishment redox– and bioaffinity–controlled elements.

The clay fraction of the examined samples is dominated by illite and illite/smectite mixed–layer phases (with 40–70 percent illite content, R=0 or R=1 type interstratification). It has been formed by preferential replacement of smectite by illite during burial diagenesis. Discrete illites seem not to be altered by heating during burial. Kaolinite is rarely found, only in samples rich in shelf–derived redeposited material. Abundance of the clay mineral species does not show any covariance with the lithology and the position in the profile. This phenomenon suggests that the processes forming the alternation of carbonate–rich and carbonate–poor semicouplets did not directly and exclusively affect the genesis of the clay minerals. Clay mineral assemblage documents erosion of smectite–rich soils developed under warm and seasonally humid climate. Sparse occurrence of the kaolinite together with the high abundance of illite and illite/smectite suggest relatively distant source area during deposition.

Stable isotope ratios of the carbonate fluctuate between 0.2 and 2.1 ‰ for carbon and between –5.1 and –0.5 ‰ for oxygen. Positive correlations were found between the measured isotope ratios of the two elements and between the isotope ratios and $CaCO_3$–content of the samples, also it can be established that carbonate–rich semicouplets are enriched in heavy carbon and oxygen isotopes in comparison with carbonate–poor semicouplets. This pattern suggests enhanced productivity, relatively 'cool' and/or 'saline' surface water during deposition of carbonate–rich semicouplets and minor role of diagenetic carbonate redistribution.

Fluctuations of P in the carbonate–rich semicouplets seem to be controlled by carbonate dilution of the terrigenous material and enhanced surface–water productivity. Diagenetic enrichment under oxic pore water conditions seems to be the most plausible explanation for relative Mn–enrichment in the carbonate–rich samples. Enrichment of the elements such as Fe, Zn, Cu, V, Ni in carbonate–poor semicouplets cannot be explained by a pure detrital source. According to Ti–normalised major and trace element enrichment factors relative to the PAAS, excess concentrations (over detrital) may be derived from seawater and could have been (at least partially) associated with the organic fraction during sedimentation. During early diagenesis moderately oxic, dysoxic conditions were favourable to decomposition of organic complexes, adsorption onto surface of the clay minerals and/or incorporation in sulfide minerals.

Rhythmic organisation of the couplets may represent palaeoenvironmental changes. Palaeoceanographic conditions alternated from efficiently mixed, high–fertility surface water and well–oxygenated seafloor (carbonate–rich beds) to enhanced runoff and/or decreased evaporation with sluggish vertical circulation and moderately oxygenated bottom water (carbonate–poor beds). This scenario should be connected to alternating anti–estuarine and estuarine circulation. The corresponding climatic conditions alternated from more arid to more humid.

Introduction

Cyclic sedimentation recorded as rhythmic lithological changes (according to terminology of EINSELE et al. 1991) in pelagic and hemipelagic sequences has been the aim of many papers in the last few decades. Interest has been concentrated on Cretaceous and younger formations, which are often characterised by cyclicity expressed as alternations of beds with fluctuating carbonate content and by minimum late diagenetic overprint as source of misinterpretations (DUFF et al. 1967, SCHWARZACHER 1975, EINSELE & SEILACHER 1982, BERGER et al. 1984, RICKEN 1991, 1994). Jurassic successions has been rarely studied (MATTIOLI 1997, BUCEFALO PALLIANI et al. 1998, COLACICCHI et al. 2000, MORETTINI et al. 2000).

The mechanisms that may produce rhythmicity or cyclicity seem to be related to the variation of environmental factors. According to several researchers (ROCC Group 1986, FISCHER et al. 1990, DE BOER & SMITH 1994, SETHI & LEITHOLD 1994, BELLANCA et al. 1996, BICKERT et al. 1997, FRANCK et al. 1999, KUMP & ARTHUR 1999, MARTINEZ et al. 1999, COLACICCHI et al. 2000, MORETTINI et al. 2000) these factors include changes (fluctuations) in

i) the supply of calcareous or siliceous biogenic sediment produced by plankton (productivity cycles);

ii) the supply of terrigenous material (dilution cycles);

iii) the degree of saturation of seawater with respect to calcium carbonate (dissolution cycles);

iv) the amount of dissolved oxygen at the seafloor and the degree of organic matter preservation (redox cycles).

Even if Milankovitch–type cyclic patterns might be expressed by a combination of physical, chemical and geological fluctuations, many of the papers emphasized so far the palaeontological aspects in order to explain the mechanisms leading to the deposition of lithological rhythms (BOTTJER et al. 1986, SAVRDA & BOTTJER 1994, ERBA & PREMOLI SILVA 1994, PITTET & STRASSER 1998). A fairly new and less common approach focuses

on the geochemical characterization of such rhythmic successions. Many works have been centered on isotope stratigraphy and organic geochemistry (WEISSERT & BRÉHÉRET 1991, JENKYNS et al. 1994, PATTERSON & WALTER 1994, BICKERT et al. 1997, BUCEFALO PALLIANI et al. 1998) and some papers used trace element geochemical data in an attempt to understand the palaeoceanographic meaning of the alternations of couplet–forming beds (MURRAY et al. 1990, 1991, 1992, 1993, MURRAY & LEINEN 1993, SUNDARARAMAN et al. 1993, BELLANCA et al. 1996). Clay minerals are known as very sensitive indicators of climatic changes in provenance and maximum heating during burial. Therefore, many authors applied clay mineral assemblage studies to determine the role of climatic, tectonic and eustatic effects in the cyclic and event stratigraphy (BISCAYE 1965, CHAMLEY 1967, CHAMLEY & DEBRABANT 1984, PACEY 1984, SINGER 1984, GYGI & PERSOZ 1986, HALLAM et al. 1991, ROBERT & KENNETT 1994, EGGER et al. 1997, GIBSON et al. 2000).

In Hungary, Triassic and Cretaceous formations from the Transdanubian Central Range have ever been analysed to describe the causes of rhythmicity and cyclicity (HAAS 1982, FOGARASI 1995). As far as the Jurassic in Hungary is concerned, description or analysis of a rhythmic or cyclic sequence was not published.

Stratigraphically uppermost part of the Fleckenmergel series named as Komló Calcareous Marl Formation (CSÁSZÁR 1997; Fig. 1) has Aalenian–Bajocian age. Its rhythmic character was first mentioned by FORGÓ et al. (1966). However, causes of the rhythmicity, causal relations between this character and possible palaeoenvironmental changes were not investigated. In this study we combine clay mineralogical and geochemical methods in order to model the palaeoenvironmental changes affecting the sedimentation of the Mecsek basin during the Bajocian.

Geological setting and lithology

The studied sections are located in the eastern part of the Mecsek Mountains (Figs 2, 3 and 4). The Mecsek Mountains belong to the Tisia Terrane, a structural megaunit of the Carpathian–Pannonian realm. According to results of research of the Apuseni Mountains (BLEAHU 1976, IANOVICI et al. 1976) and of the Great Hungarian Plain (BALÁZS et al. 1986, GROW et al. 1994), the Tisia Terrane is a basement nappe system overthrust with northern vergency during the Cretaceous Austroalpine tectogenesis.

In the Jurassic the area was part of the northern continental margin of the Tethys. Differentiation of the carbonate shelf into extensional structures started during the Late Triassic (NAGY 1969). This

process has continued in the Early Jurassic as a result of rifting of the Penninic Ocean. Early Liassic is characterised by a continental and shallow marine sequence with arkose–type sandstones and coal measures (Gresten facies). The overlying sequence is usually compared with the Allgäu facies of the Northern Alps. Dominant lithofacies is abundant spotted, bioturbated marl and siltstone intercalated by mixed carbonate–siliciclastic turbidites, crinoidal limestones and interrupted by a black shale horizon in the Early Toarcian. This type of sedimentation prevailed until the Late Bajocian. The whole Jurassic succession up to the Bajocian *Strenoceras niortense* Zone developed to a maximum thickness of 3700 m.

Age		Mecsek Mts.
Malm	Tithonian	+ Márévár + Limestone Fm.
	Kimmeridgean	Kisújbánya Limestone Fm.
	Oxfordian	Fonyászó Limestone Fm.
Dogger	Callovian	Dorogó C. Marl Fm.
	Bathonian	Óbánya Limestone Fm.
	Bajocian	Komló C. Marl Fm. 3.
	Aalenian	
Lias	Toarcian	Óbánya Aleurolite Fm.
	Pliensbachian	2. 1. Hosszúhetény C. Marl Fm.
	Sinemurian	Vasas Marl Fm.
	Hettangian	Mecsek Coal Fm.

Fig. 1. Jurassic lithostratigraphic units of the Mecsek Mountains (CsÁSZÁR 1997). 1. Kecskehát Limestone Formation; 2. Mecseknádasd Sandstone Formation; 3. Pusztakisfalu Limestone Formation.
Different facies types are indiced as follows: coal swamp: symbolic plants; hemipelagic bioturbated marl: waves; crinoidal limestones: brickwall pattern; micritic pelagic limestones: crosses.

Two outcrop profiles north of village Püspökszentlászló belonging to the Komló Calcareous Marl Formation (Fig. 1) were studied in detail. They are named as Püspökszentlászló II, and Kecskegyűr, road cut (Fig. 4). They represent an Early to Middle Bajocian succession indicated by a *Kumatostephanus* sp. (GALÁCZ 1997, pers. comm.) found on the base of the succession. The 53.87 m thick section consists of an alternation of carbonate–rich and carbonate–poor layers with couplet character. The thickness of individual carbonate–rich layers alternates between 12 and 78 centimetre. Carbonate–poor beds have a minimum of 9 and a maximum of 106 centimetres bed thickness. Sharp and continuous bedding contact can also be observed. Macroscopic sedimentary structures indicating redeposition by gravity mass flows or contourites do not appear. Hardgrounds and other features of submarine dissolution and sediment starvation were not detected on the sharp bedding contacts.

The beds are grey and greenish grey (with some yellowish shade on the weathered surfaces) with abundant darker grey spots. All beds are macroburrowed, microburrowing is absent. The carbonate–rich beds are massive and characterised by conchoidal fracture. Carbonate–poor semicouplets are less massive, they can be easily splitted into 1–2 centimetre thick 'sublayers'. Fine and graded lamination do not appear.

According to thin section analyses the rocks are classified as bioclastic packstone and wackestone. The most abundant biogenic components of the carbonate–rich semicouplets are round–shaped calcified molds without any inner structures and filaments. A few radiolarian tests are not recrystallized. These microfossils may suggest radiolarian origin of the calcite–filled molds. Carbonate–poor beds are dominated by siliceous sponge spiculae. Echinoid fragments up to 10 percent of total bioclastic assemblage were found almost in all samples. Foraminifers are present in some thin sections. *Lenticulina* sp., *Spirillina* sp. and *Garantella* sp. cannot be used for dating but they suggest normal marine salinity (RESCH 1997, pers. comm.). Up to 5 percent of unrounded terrigenous quartz silt and very fine sand grains (with 0.02–0.09 mm maximum diameter) are present as well. Mica flakes (up to 0.5–0.6 mm) commonly present on bed surfaces in the case of carbonate–poor semicouplets.

Features indicating redeposition and erosion by gravity mass flow or contourite activity (gradation, graded and cross lamination, lenticular bedding, presence of fine, obscure silt lenses, complete or incomplete Bouma–sequence) were not observed in the thin sections, and the bioturbation is widespread. The partial dissolution and recrystallization of some biogenic constituents indicate carbonate and silica dissolution–reprecipitation processes during burial diagenesis. However, stylolites and other dissolution–related discontinuity surfaces do not appear Wavy bedding surfaces are widespread, nevertheless carbonate concretions have not been formed, i. e. diagenetic carbonate redistribution in the sense of HALLAM (1964) probably was not significant enough to cause this limestone/marl alternation.

In essence, the studied profiles represent basinal facies dominated by hemipelagic processes. Sedimentation seems to be presumably continuous. Consequently, this succession is a good candidate for detailed analysis to examine the origin of rhythmic bedding.

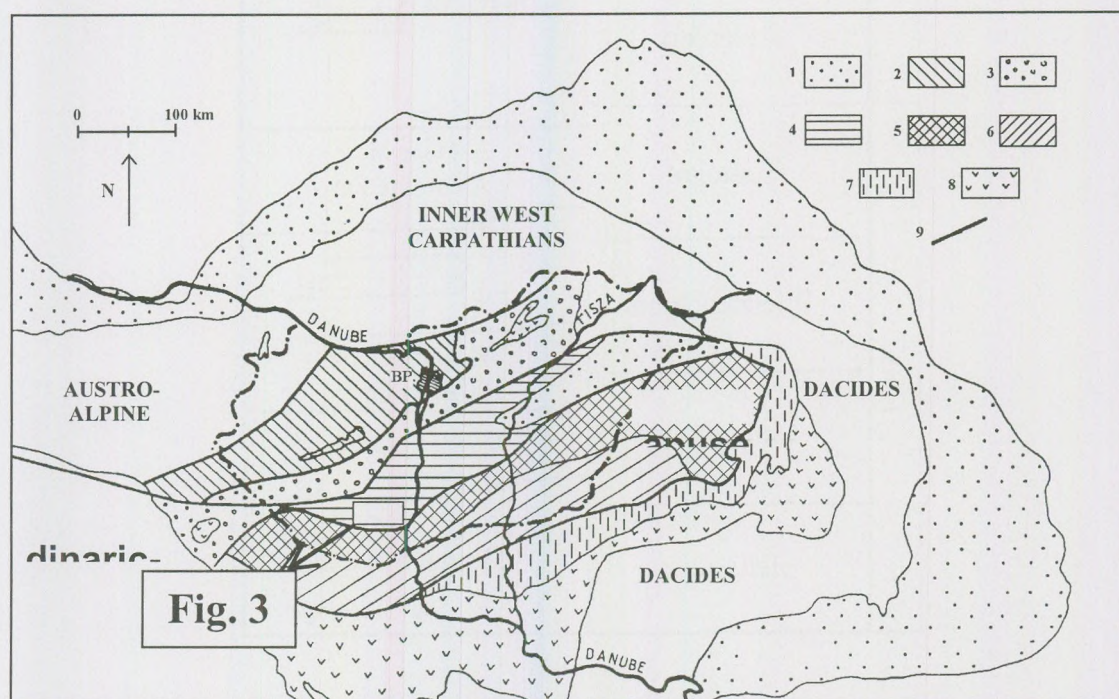Fig. 2. The location of Mecsek Mountains in the Mesozoic tectonofacial units of Hungary, modified after TÖRÖK (1997a). 1. Foredeep and flysch units; 2. Transdanubian and Drauzug units; 3. Bükk and Inner Dinaric units; 4. Mecsek unit (area of the Mecsek Mts. is indicated by gray rectangle); 5. Villány–Bihor unit; 6. Papuk–Lower Codru unit; 7 N. Bačka–Upper Codru unit; 8. Oceanic nappes; 9. Boundaries of tectonofacial units
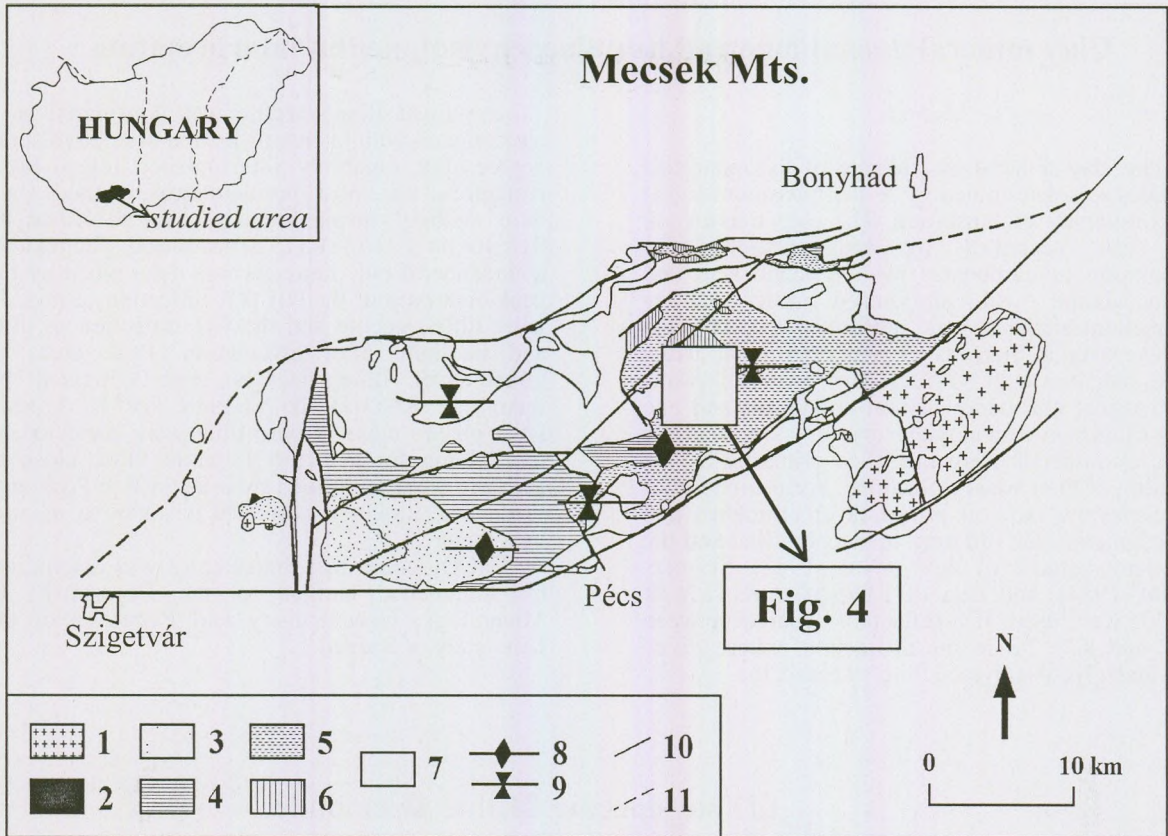
Fig. 3. Geological map of the Mecsek Mountains, simplified after TÖRÖK (1997b).
1 Carboniferous granite; 2. Permian rhyolite; 3. Upper Permian; 4. Triassic; 5. Jurassic; 6. Cretaceous; 7 Post–Cretaceous; 8. anticline; 9. syncline; 10. fault; 11. supposed fault.
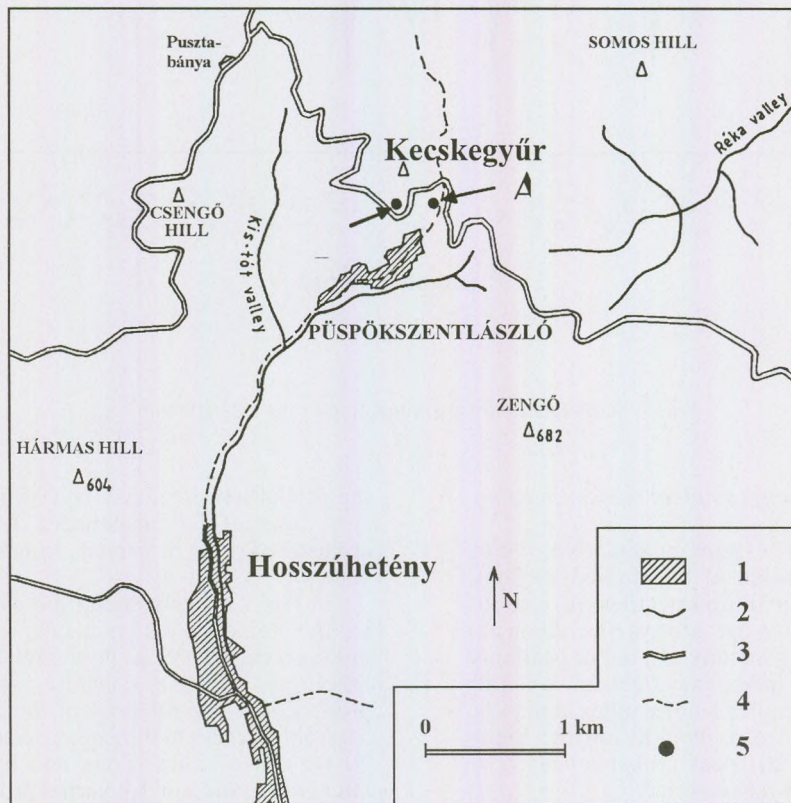

Fig. 4. Location map of the two examined sections. 1. settlement; 2. creek; 3. road; 4. path; 5. location of the examined sections; A: section Püspökszentlászló II; B: section Kecskegyűr, road cut.

Clay mineral assemblage and its palaeoenvironmental interpretation

Methods

The clay mineral assemblage of the examined samples was determined by X–ray measurements at the University of Innsbruck. The clay fraction <2 μm was separated by sedimentation after dissolution of carbonates by 3% acetic acid and deflocculation with desionized water. X–ray diffraction analysis was performed on oriented pastes, with a Siemens D–500 instrument using CuK$_\alpha$ radiation with Ni filter. Two X–ray diagrams were made: one under natural conditions and one after saturation with ethylene glycol.

Clay minerals were identified primarily by the position of their basal reflections. For estimation of illite/smectite ratio in mixed–layer structures and for estimation the ordering of interstratification the standard methods of WATANABE (1981), ŚRODON (1980, 1984), and data of REYNOLDS & HOWER (1970) were used. If a reflection occured between 5.3° and 8.7° 2Θ in the diffraction pattern of an ethylene glycol–solvated illite/smectite, the examined illite/smectite was considered as a clay mineral with interstratification ordered to some degree. For randomly interstratified mixed–layer structures, the most problematical method ('a/b ratio method') using intensity data published by REYNOLDS & HOWER (1970) was used. The relative abundance of clay minerals was determined by the peak area ratio of the 001/001 reflection of mixed–layer illite/smectite and the 001 reflection of illite and kaolinite after glycolation. Peak areas of mixed–layer illite/smectites were corrected by factors of RISCHÁK & VICZIÁN (1974). Mixed–layer phases close to pure illite were corrected by multiplying by a factor 2, while those close to smectite were multiplied by a factor 0.5. Peak area of discrete illite was corrected in a similar manner by a factor 2.

CaCO$_3$–content of the samples was determined by volumetric method at the Department of Mineralogy, Geochemistry and Petrology of the University of Szeged.
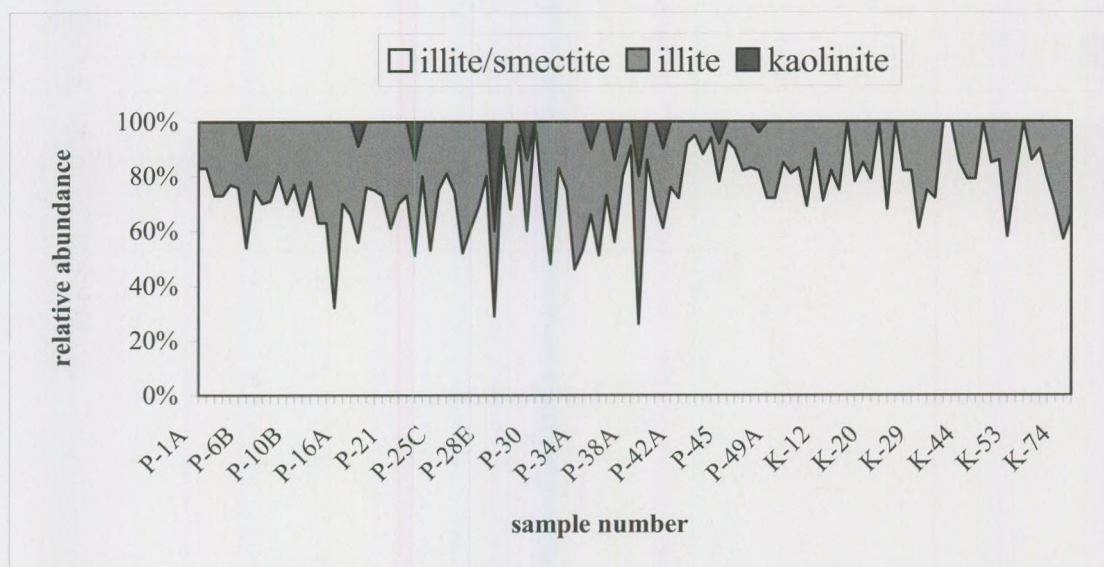
Fig. 5. Semi–quantitative composition of the clay fraction

Results of the clay mineralogical measurements

Fig. 5 shows semi–quantitative clay mineralogical composition of the studied sections. Illite and mixed–layer illite/smectites of various degree of expandability are always the dominant clay minerals. Illite is generally of poor crystallinity (values of the Kübler index vary between 0.6–1.0° 2Θ). In most of the samples Kübler index cannot be exactly measured due to a shoulder on the high–angle side of the illite 001 peak probably caused by the expanded mixed–layer phases.

The relative abundance of the mixed–layer phases in function of the CaCO$_3$–content of the samples is plotted in the Fig. 6. It is obvious that the proportion of mixed–layer illite/smectite in the clay fraction is independent from the CaCO$_3$–content of the measured samples (see the "*r*" values).

In Fig. 7 the estimated illite percentage intervals in the mixed–layer minerals are shown. It is obvious that there is no correlation between the lithology (CaCO$_3$–content) and the illite proportions. The majority of the examined mixed–layer illite/smectite minerals is characterised by 40–70 percent of illite layers and by mostly random interstratification or 1/4 partial ordering.

Kaolinite appears seldom (10% of all the measured samples), mostly in low amount (14.3% average abundance; maximum value = 40% in

sample P–29A) and only in the carbonate–rich semicouplets (Fig. 5). However, there is no correlation between the $CaCO_3$–content of the samples and the abundance of this clay species (r =–0.2071) (Fig. 8).
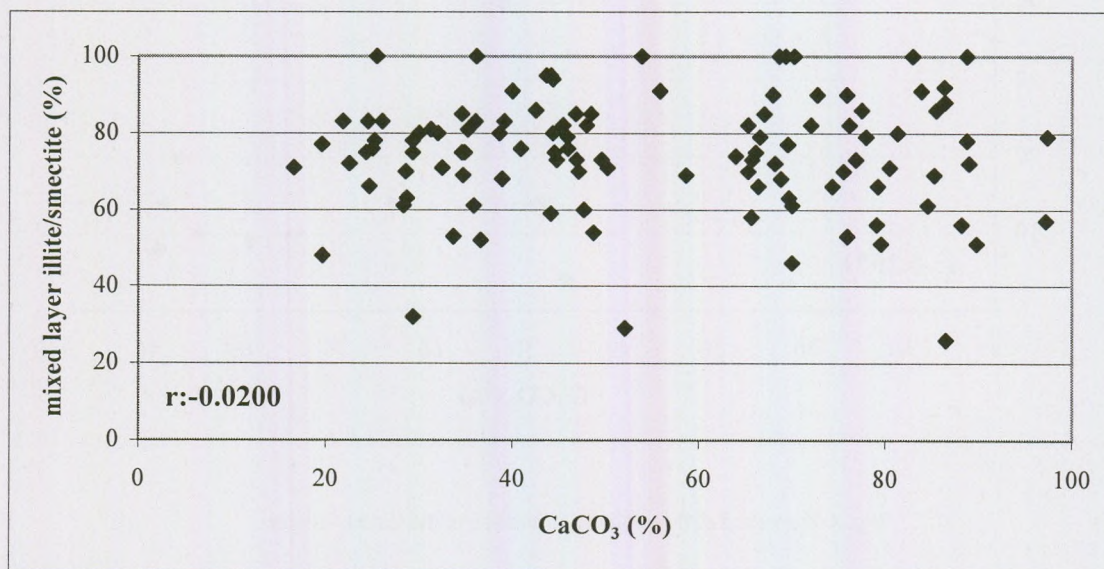
Fig. 6. Proportion of the illite/smectite mixed–layer minerals in function of the $CaCO_3$–content
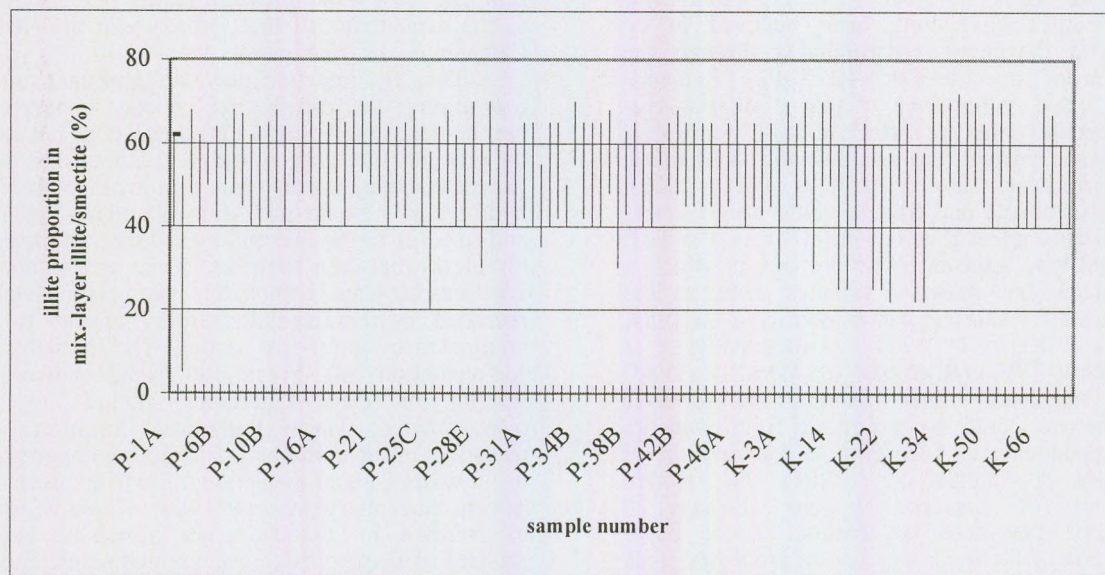
Fig. 7 Estimated illite proportion of the mixed–layer illite/smectite clay minerals

Discussion

In most regions of the world ocean, clay detrital assemblages reflect the combined influences of land petrography and continental climate (BISCAYE 1965). The common clay minerals used as environmental indicators are kaolinite, mixed–layer illite/smectite and illite.

In the modern oceans kaolinite abundance increases toward the Equator in all oceanic basins and therefore expresses a strong climatic dependence controlled by the intensity of continental hydrolysis. In modern marine sediments, kaolinite tends to increase in relative abundance in neighbouring regions of tropical continental weathering. The strong increase in kaolinite (together with goethite, gibbsite) could reflect very intensive weathering on the source area (CHAMLEY 1989, ROBERT & KENNETT 1994, GIBSON et al. 2000). As for Jurassic formations in the Mecsek Mountains, NAGY (1969), VICZIÁN (1987) reported high amount of kaolinite in the Mecsek Coal and Vasas Marl Formation.
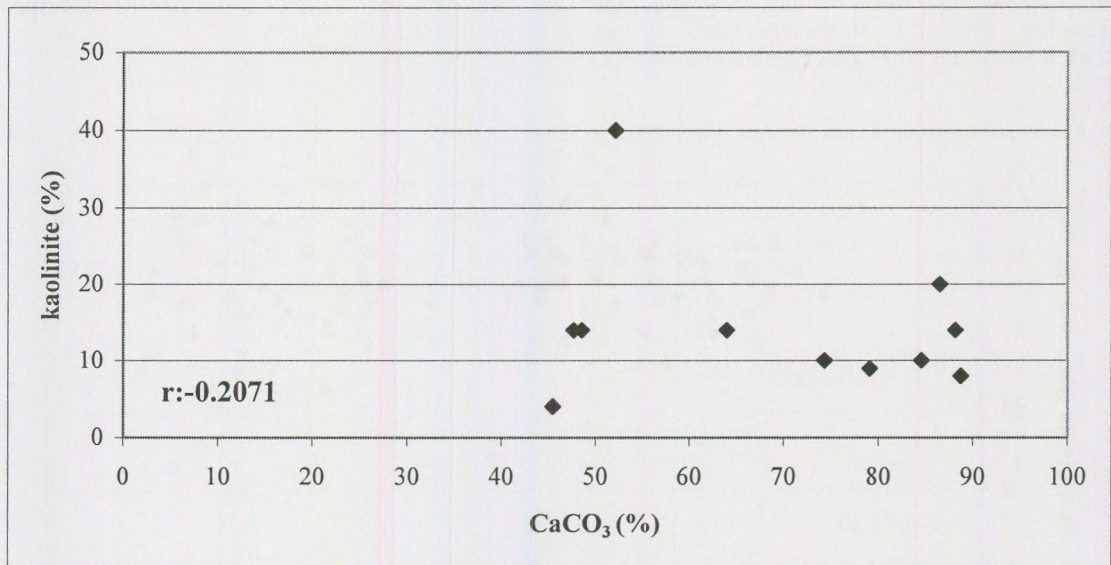
Fig. 8. Proportion of the kaolinite in function of the CaCO₃–content

The distribution of mixed–layer minerals in the present day oceans have strong geographic controls. This indicates continental sources rather than in situ diagenetic origin (BISCAYE 1965). Mixed–layer illite/smectites have long been believed to be formed in diagenetic environments through the alteration of smectite (HOWER 1981). Evidence does exist, however, that mixed–layer illite/smectites may form in a weathering environment through the leaching and degradation of a precursor illite (CHAMLEY 1967, 1989). Although smectite and illite/smectite mixed layers form recently under a variety of climates, the most important type appears to be the one in which a pronounced dry season alternates with a less pronounced (or shorter) wet season (SINGER 1984, ROBERT & KENNETT 1994, VANDERAVEROET & DECONINCK 1997). ROBINSON & WRIGHT (1987) have suggested that some mixed–layer illite/smectite could be produced from smectite during pedogenesis. According to the opinion of CHAMLEY & DEBRABANT (1984) the relative abundance of smectite largely displays a distribution that does not parallel to the zonal distribution of the main weathering processes. This could indicate the accessory control of climate and the dominance of other processes. The increase of Al–Fe–rich smectites and their abundance does not depend on deposition in marine environment but are chiefly attributed to the reworking of continental peneplanation of gently sloping and poorly drained areas. It must be noted that smectite may be entirely volcanogenic in origin, being derived directly from the weathering of lava or volcanic ash and tuffs, and thus having nothing to do with climate. In this case, however, distinctive accessory minerals must occur, such as biotite, sphene, cristobalite, zeolites and, rarely, relict glass shards (PACEY 1984, ÇELIK et al. 1999).

The occurrence of discrete illite in sediments probably has no particular climatic significance (HALLAM et al. 1991, ROBERT & KENNETT 1994), but SINGER (1984) claims that illite exhibiting high

crystallinity signifies formation in either cold or dry conditions with minimum hydrolysation. Because of low crystallinity of illite in the measured samples, these conditions can hardly be considered as the explanation of their presence in the Komló Calcareous Marl Formation.

Differential transport plays an important role in determining the distribution of clay minerals in marine deposits. As early diagenesis does not seem to account for such a differentiation, one may expect that clay sorting was reinforced both by a hydrolysing climate providing abundant kaolinite and smectite to the sea, and by sudden variations of turbulence between shelf and basin environments. The mechanisms responsible for clay changes recorded on continental margins appear to be dominated by grain size sorting. The influence on sedimentation of direct and rapid subvertical sinking of clay aggregates should not be overestimated, since horizontal transport and resuspension of individual particles and aggregates occur widely, under the action of surficial, deep and bottom currents (CHAMLEY 1989). Kaolinite tends to increase in abundance in nearshore facies, probably reflecting its coarse–grained nature and its strong tendency to flocculate compared to most other clays (PARHAM 1966). Clay sorting usually determines the farther transportation of smectite and fibrous clays relatively to the most other clay species.

The sparse occurence of kaolinite in the rocks of the Komló Calcareous Marl Formation is restricted to a few carbonate–rich semicouplets rich in shelf–derived bioclasts. According to micropaleontological data there are Ostracods in the Komló Calcareous Marl Formation collected from other locations of Mecsek Mountains, which indicate shallow–water environment and certainly have resedimented from the platforms (MONOSTORI 1997, pers. comm.). These data suggest resedimentation from the neighbouring shallow shelf areas. However, based on the field and microfacies observations, presence of gravity mass

flows is not evidenced in the studied succession. Extreme low density turbidites, nepheloid plumes or slow bottom currents could cause this type of resedimentation (TUCKER & WRIGHT 1990).

Another complication concerns diagenesis. Under conditions of increased temperature due to burial, smectite tends to transform to illite via an intermediate stage of mixed–layer minerals (HOWER et al. 1976). In the Hungarian literature VICZIÁN (1994) has summarized the application of the illite–smectite geothermometry. According to his paper the intensity of smectite–to–illite transition depends on the variables time, temperature, K^+ availability in the depositional environment and activation energy. He has presented an illite proportion in mixed layer structure versus maximum burial temperature trend line calculated from data of Pannonian Basin. Part of this line corresponding to 40–70% smectite in mixed–layer indicates 100–130°C heating temperature during burial diagenesis. According to fission track data presented by DUNKL (1992) a range of 100–175°C burial heating temperature was estimated in the case of the Jurassic sequence in the eastern part of the Mecsek Mountains. According to VICZIÁN (1990) illite contents in the mixed–layer phases of the underlying Mecsek Coal and the Vasas Marl Formations are 70–80%. This higher illite content – thus higher crystallinity – is due to deeper burial and higher degree of 'ripening' of illite/smectite phases in accordance with the deeper stratigraphic position of these Early Jurassic formations.

PARRISH et al. (1982), HALLAM (1984), KUTZBACH & GALLIMORE (1989) declared in agreement with each other, that both modelling and empirical research suggest that zonal winds were probably much less important on the Jurassic supercontinent than monsoonal winds. It seems evident that temperature was higher than recently, dry and wet seasons were alternating during these monsoon–controlled times. According to HALLAM et al. (1991) the pronounced increase in smectite abundance of the latest Jurassic rocks from England and France signifies a climate with a more pronounced and extended dry season in contrast that in the Cretaceous. Results of simulations presented by CHANDLER et al. (1992) show that increased ocean heat transport may have been the primary force generating warmer climates during the Early Jurassic. Three major features of the simulated Jurassic climate include the followings:

i) A global warming, compared to the present;

ii) Decreases in albedo, occurring because of reductions in sea ice, snow cover, and low clouds, and increases in atmospheric water vapour are the positive climate feedbacks that amplify the global warming;

iii) High rainfall rates are associated primarily with monsoons that originate over the warm Tethys Ocean.

These systems are found to be associated with localised pressure cells whose positions are controlled by topography and coastal geography. WEISSERT & MOHR (1996) studied carbon isotope composition of large amount of limestone samples representing the Oxfordian–Tithonian interval from the Helvetic nappes. They concluded that the climate in the northern Tethyan realm has been characterised by high atmospheric CO_2 level and by monsoonal rainfall pattern. No observation has been suggested so far that in the Bajocian stage in the Mecsek sedimentation basin climatic conditions were different.

Palaeoenvironmental interpretation

Dominance of illite/smectite mixed–layer phases indicate seasonally alternating monsoon–like climatic conditions during the Bajocian in the source area of the Mecsek sedimentary basin. Under this weathering condition, pedogenic smectite and/or disordered mixed–layer illite/smectite has been formed and carried into the basin. 40–70% illite proportion in mixed–layer and the moderate ordering are due to diagenesis and indicate 100–130°C heating temperature during burial. Discrete illites were not influenced by heating of such a degree. The sparse occurrence of kaolinite and abundant mixed–layer phases besides of illite and absence of chlorite can suggest a relatively distant source area during deposition.

Kaolinite was poor and were found only in limestone samples. Diagenetic alteration of kaolinite to illite or to chlorite (CHAMLEY 1989) can be excluded because of 100–130°C burial temperature suggested by mixed–layer illite/smectites (HUANG 1993). The following explanations can be reliable:

i) Morphological barriers or well–developed river–fed marginal basin existed which would prevent the carry into the ocean many of minerals pedogenically formed in the upstream zones;

ii) The kaolinite was resedimented by sporadic nepheloid plume activity and/or bottom currents from the neighbouring shallow–water shelf areas.

The clay mineral types do not correlate qualitatively and quantitatively with the lithologies. This observation suggests that processes forming the limestone/marlstone alternation could not affect exclusively the formation of the clay minerals.

Stable O– and C–isotope geochemistry

Determination and interpretation of stable isotopic composition of carbonate rocks have been extended during the last few decades. This geochemical method is preferentially used in palaeogeographic, palaeoclimatic and palaeo–ecologic modeling of rhythmic and cyclic sequences (KUMP 1989, LASAGA 1989, POPP ET AL. 1989, MAGARITZ & HOLSER 1990, GROSSMAN et al. 1991, 1993, LAFERRIERE 1992, HOLLANDER et al. 1993, LONG 1993, BARRERA & KELLER 1994, PELECHATY et al. 1996, WENZEL & JOACHIMSKI 1996, JOACHIMSKI et al. 1998, CAPLAN & BUSTIN 1999, FRANCK et al. 1999, JACOBSEN & KAUFMAN 1999, KUMP & ARTHUR 1999, PROKOPH & VEIZER 1999, MORETTINI et al. 2000).

The background process is that from sea– or porewater precipitated (biogenic, sedimentary or diagenetic) calcite can be enriched in heavy oxygen with 18 mass number. Degree of the enrichment is controlled by temperature and salinity of the water, therefore fluctuations in $\delta^{18}O$ of carbonate rocks show well changes in temperature and/or salinity of a given part of the water column or in temperature and/or salinity of the pore water. Diagentic carbonate dissolution and reprecipitation can be also recorded in oxygen isotopic composition (O'NEIL et al. 1969; FRIEDMAN & O'NEIL 1977).

Fluctuations in carbonate and organic $\delta^{13}C$ are widely used for modelling of changes of marine organic productivity and coexisting redox changes, because increased productivity causes relative enrichment of seawater in heavy carbon isotope due to preferred uptake of light carbon by phytoplankton during photosynthesis. However, long–term excursions of $\delta^{13}C$ during Earth's history seem to be caused by several other factors such as degree of weathering and burial fluxes of the carbon (intensity of carbon recycling) and evolutional state of the biosphere (KUMP 1989, LASAGA 1989, POPP et al. 1989).

In the Hungarian literature, the stable isotope approach in sedimentological and cyclo–stratigraphical research has been presented sporadically (CORNIDES et al. 1979, FOGARASI 1995). While the Komló Calcareous Marl Formation shows obvious rhythmic character, application of the stable isotopic method can be effective in the examination of the rhythmicity–forming factors.

Methods

25 bulk samples were milled in an agate mortar and the powder was analysed at the Geochemical Research Laboratory of the Hungarian Academy, Budapest. Carbon dioxide was produced following MCCREA (1950)'s standard method. The $^{13}C/^{12}C$ and $^{18}O/^{16}O$ ratios were determined using a Finnigan MAT Delta S mass spectromether. The isotope ratios are quoted in per mil relative to the PDB (Pee Dee Belemnite). The reprodubilicity of duplicate analyses is better than ± 0.1‰. The standard Harding Iceland Spar was also analysed, which yielded the following values:

$\delta^{13}C$: –4.88 ± 0.03 ‰; $\delta^{18}O$: 11.85 ± 0.07 ‰; n: 4. (Accepted values: $\delta^{13}C$: –4.80 ‰; $\delta^{18}O$: 11.78 ‰; LANDIS 1983)

The samples are collected from couplets. Only unweathered and hypergene transformation–free specimens were selected for the stable isotope analysis.

Results

Stable isotope data of the examined samples are collected in the Table I. Summarizing the following can be established:

i) In a given couplet, the $CaCO_3$–rich layers are isotopically heavier for both elements than the $CaCO_3$–poor ones.

ii) Relative strong correlations exist between the $CaCO_3$–content and the $\delta^{13}C$ and the $\delta^{18}O$ values (Figs 9 and 10).

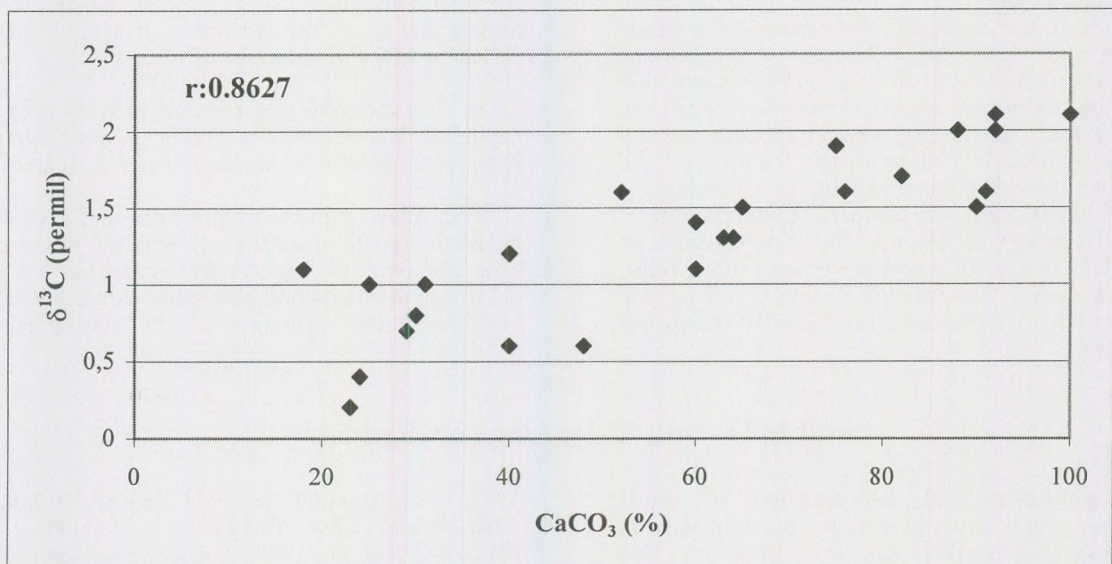iii) The $\delta^{13}C$ and the $\delta^{18}O$ values are corresponding to the 'normal' pelagic real.

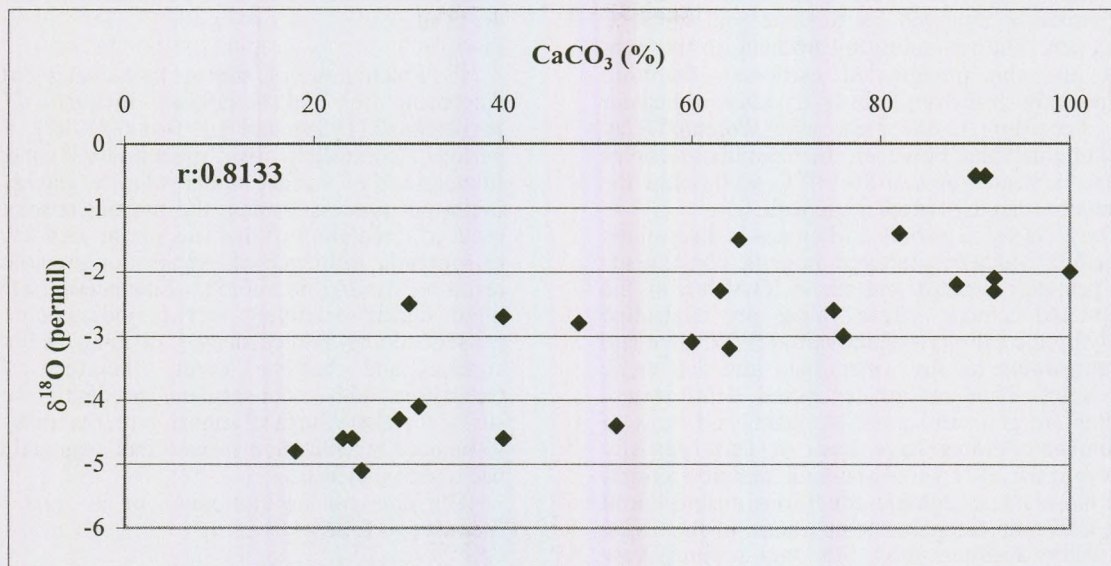Fig. 9. Carbon isotope ratios versus $CaCO_3$–content diagram

CaCO$_3$ (%)

Fig. 10. Oxygen isotope ratios versus CaCO$_3$–content diagram

Discussion

ARTHUR et al. (1984, 1986) proposed that periodic changes of insolation, evaporation, wind stress, and/or rainfall in a wide variety of environments were able to cause changes of input of terrigenous matter, water mass stratification, deep–water oxygenation, surface water productivity and related chemical, biological, ecological factors. These changes could be very effective in the case of the intrashelf basins due to their small volume of water mass relatively to the oceanic realm. In contrast to the well documented Pleistocene and Holocene situation, changes in ratio of deep–water production during glacial–interglacial transitions and related changes in carbonate dissolution probably cannot be accounted for explain the rhythmic alternation of Jurassic sequences deposited during greenhouse conditions. Some of the above mentioned changes can be traced by stable isotopic data.

The examined samples contain carbonate fossils, abundant micritic matrix (primary and/or diagenetic) and diagenetic calcite spar–filled molds. The carbon isotopic composition of these constituents reflects the composition of the dissolved bicarbonate of the water from which their matter is precipitated. Main factors controlling of the carbon isotope signal are as follows:

The seawater surface is usually enriched in ^{13}C relative to the deep water (BERGER & VINCENT 1986, THUNELL et al. 1991, BELLANCA et al. 1995, 1996) which invokes ^{13}C enrichment of carbonate–secreting zooplankton as a result of an increase in productivity of phytoplankton. BARTOLINI et al. (1996) described positive δ^{13}C excursions in Early Bajocian and Callovian–Oxfordian carbonate rocks in Italy that may record changes in global climate toward warmer, more humid periods with increased carbon burial and nutrient mobilisation. Many

workers emphasized that increased radiolarian abundance in sedimentary successions appears parallel with increased δ^{13}C values and other high productivity–related palaeontological and geochemical features (FÖLLMI et al. 1994, BILL et al. 1995, BARTOLINI et al. 1996, 1997, JENKYNS 1996, BARTOLINI & GUEX 1999, COLACICCHI 2000). In many cases, drastic shifts were found in global δ^{13}C pattern. However, these shifts do not show clear correlation with diagenesis– and productivity–related properties of the examined successions. For example, MII et al. (1997) pointed out that the very high δ^{13}C values of the Permian Svedrup Basin seems to be correlated the globally recognized δ^{13}C shift explained by changes in the size of the global organic carbon reservoir (KUMP 1991). Other plausible explanation of such drastic carbon isotope shifts is changes of the absolute amount of carbon dioxide in the ancient atmosphere (MARSHALL & BRENCHLEY 1998, PANCOST et al. 1998).

Diagenesis may alter the carbon isotopic composition of sedimentary rocks. However, this composition does not change a great deal during diagenesis because the volume of carbon within the pore–water reservoir is small and because the isotope fractionation between calcium carbonate and dissolved bicarbonate is small at low temperatures (EMRICH et al. 1970). JENKYNS & CLAYTON (1986) proposed a model to explain the very low δ^{13}C values associated to organic–rich sedimentary rocks in the Tethyan Lower Jurassic. In their model the lower δ^{13}C of the cement is compatible with the introduction of carbon dioxide derived from bacterial (anaerob) oxidation of organic matter According to RAISWELL (1987), during sulfate reduction and bacterial decomposition of organic matter lead to precipitation of ^{13}C–depleted calcite. RICKEN & EDER (1991) emphasize that with increasing

overburden, the sediment passes into the methane production zone, where isotopically light bicarbonate is removed by the bacterial methane production. The remaining bicarbonate in the pore water and the precipitated carbonate therefore continuously shift from light $\delta^{13}C$ values to heavier ones. According to the previously presented clay mineralogical data, however, the examined samples seem to be heated up to 100–130°C, well below the temperature range of methanogenesis.

The $\delta^{18}O$ value of bulk carbonates is determined by the $\delta^{18}O$ value of unaltered biogenic constituents (and primary micrite) and the $\delta^{18}O$ value of the precipitated cement. These values are controlled mainly by the salinity–related initial $\delta^{18}O$ value and the temperature of the water mass and diagenetic pore water. Thus, at greater burial depth where cements are generally more abundant and most of the biogenic grains have been at least partially dissolved, the $\delta^{18}O$ values of bulk samples reflects more closely the geologic conditions during burial diagenesis than the palaeotemperature of the initial sea water shifting those to the progressively negative values (KILLINGEY 1983, COOK & EGBERT 1983). Highly negative oxygen isotope values are formed in freshwater–related and at high temperature precipitated carbonates. During diagenesis, oxygen isotope ratios are likely to be far more readily altered than carbon isotope ratios. The ratio of oxygen in pore water to oxygen in the rock in initially extremely porous carbonate oozes is high, the inverse is true with respect to carbon. In addition, there is a large temperature fractionation of oxygen isotopes which can play an important role during burial diagenetic cementation. Such effects have been noted in many pelagic sequences (SCHOLLE 1977). According to EINSELE & RICKEN (1991) the oxygen isotopic composition of marl and limestone beds of the rhythmic marl/limestone alternations may be homogenized by diagenetic processes.

There are several stable isotopically well studied sequences of ice–free periods of the Earth's history (WEISSERT et al. 1979, DE BOER 1983, KAUFFMAN 1988). According to these authors, two mechanisms should be considered to explain the relatively low oxygen isotope values of the carbonate of the marly (carbonate–poor) beds of such rhythmic pelagic–hemipelagic sequences:

i) Fluctuation of the surface water temperature. The temperature of the sea surface is controlled not only by the temperature and circulation of the atmosphere. In the zones characterised by intensive upwelling, oxygen isotopically heavy bottom water might have reached the photic part of the water column, therefore here carbonate secreting organisms might have formed carbonate skeleton

with relatively high $\delta^{18}O$ values. In these cases the main controlling factor is the circulation pattern of the basin.

ii) Fluctuation of the surface water salinity. According to PRATT (1984), BARRON (1986), KAUFFMAN (1988) and DE BOER (1991), during periods controlled by greenhouse conditions fluctuations of surface water salinity was a more important process than in the present oceans. The reduced circulation of the seas might well have led to a greater influence of evaporation/precipitation, resulting a variable salinity. Enhanced freshwater input during relatively wet periods could have caused salinity–related density differences between surface and bottom water, therefore slower circulation and lower organic production in the surface water. Surface runoff patterns may have influenced stratification in marginal seas and could had a global effect.

Our data can be interpreted in the light of the literature as follows:

i) During deposition of the carbonate–rich layers characterised by high $\delta^{13}C$ values, surface water productivity seems to be increased relatively to the carbonate–poor semicouplets. This is in accordance with the observed radiolarian abundance: microfacies of the carbonate–rich semicouplets are dominated by recrystallized radiolarian tests.

ii) According to ARTHUR & DEAN (1991), $\delta^{18}O$ values –2.5 to –4.5 ‰ are reasonable isotopic composition for diagenetically marine carbonates formed in a warm, ice–free sea. Most of our samples have $\delta^{18}O$ values within this range.

iii) The carbonate–rich layers are isotopically heavier. If diagenetic carbonate redistribution had been the main factor in form the rhythmic character of the sequence, an opposite trend would have been observed. 1.5 to 2.5 ‰ difference between $\delta^{18}O$ values of the neighbouring beds also contradicts the dominance of the diagenetic redistribution.

iv) The above mentioned fluctuation in the $\delta^{18}O$ pattern points to differences in temperature and/or salinity during the sedimentation. Carbonate–rich beds seem to be formed during periods of 'cooler' and/or 'more saline' surface water.

v) However, redeposition of platform–derived shallow water carbonate mud by bottom currents and/or by nepheloid plume activity cannot be exluded as potential source of isotopically (for both measured elements) heavy carbonate.

Major and trace element geochemistry

Geochemical characterization of the rhythmic and cyclic sequences was mainly focused on stable isotopic composition of the examined material. Major and trace element examination of sediments and sedimentary rocks has served provenance studies and analysis of the weathering processes (NESBITT & YOUNG 1982, BHATIA 1983, HARNOIS 1988, ROSER & KORSCH 1988, NESBITT et al. 1997,

HUISMAN et al. 2000, VALLADARES et al. 2000, VARGA et al. 2001). In the past decade, however, interpretation of the element composition of rhythmically alternated biogenic sediments went an effective tool in modelling of (i) changes of seawater chemistry (ELDERFIELD 1990, DYMOND et al. 1992, FILIPELLI & DELANEY 1996); (ii) environmental factors of biogenic sedimentation

(SCHMITZ 1987, YAMAMOTO 1987, MURRAY et al. 1991, 1992, SUNDARARAMAN et al. 1993, FAGEL et al. 1997, ZWOLSMAN et al. 1997, REYNARD 1998, ZHANG et al. 2000); (iii) rhythmicity–forming mechanisms in marine successions (LYLE et al. 1988, ABOUCHAMI et al. 1997).

Methods

45 samples were collected from six intervals of the studied succession to determine of their chemical composition by PIXE analysis. The name PIXE (Particle Induced X–Ray Emission) refers to a process in which characteristic X–rays are generated by ion–atom collision events as the consequence of the recombination of electron vacancies appearing in the inner shells. The spectroscopy of X–rays reveals analytical information on the elemental constituents of the samples. In such a way multielemental analysis with low detection limit can be performed on thin and thick samples of small absolute mass (JOHANSSON 1988).

The 2 MeV energy proton beam of the 5 MeV Van de Graaff accelerator of the Institute of Nuclear Research of the Hungarian Academy of Sciences, in Debrecen has been used for PIXE analysis. Details on the experimental setup and its calibration have been given in BORBÉLY–KISS et al. (1985) as well as in SZABÓ & BORBÉLY–KISS (1993). Powdered bulk rock samples were pressed into pellets (1 mm thick and 10 mm in diameter). The beam current was typically between 1 and 10 nA, with a beam size of 5 mm in diameter and about 20 minutes bombardment was sufficient to detect elements in the sample. Spectra have been evaluated with the PIXYKLM programme package (SZABÓ & BORBÉLY–KISS 1993).

Standard deviations given in the tables include the statistical errors originating from the measuring conditions and the fitting of X–ray spectra. However, they do not include the error of data necessary for the determination of elemental concentrations. Those data (X–ray production cross section, respond probability of the Si(Li) detector, X–ray absorption in the sample and the used filter and the slowing down of proton beam in the sample) are calculated theoretically. Errors of those data are systematic, depend on the atomic number and can only be estimated. They are less than 10–15 % of the value of concentrations.

Results

Major and trace element data are listed in Tables II and III. Average values of the measured elements of the carbonate–rich semicouplets are indicated by 'average 1'; 'average 2' indicates those of the carbonate–poor beds. Values with higher than 10% standard deviations are indicated by bold numbers. Missing values in the Tables II and III mean that the concentrations of those elements are less than the detection limit. Calculated correlation matrix is presented in Tables IV and V. shows the Ti–normalised enrichment factors relative to the PAAS values for many elements (TAYLOR & MCLENNAN 1985) calculated as follows:

$$(El/Ti)_{sample}/(El/Ti)_{PAAS}$$

where *El* refers to any measured element.

Tables of DOWDY & WEARDEN (1983) were used for statistical evaluation of data.

Discussion

While the studied rocks are fine–grained mixed carbonate–siliciclastic rocks, calcite– and phyllosilicate–related elements have been found as major constituents.

Two main sources of the silicon are the biogenic opal and the terrigenous matrial (quartz and silicate minerals). Si shows slight positive correlation with the titanium ($r=0.700$, $n=25$) that clearly indicates contribution of the terrigenous fraction to the total Si concentration. According to results of the microfacies analyses almost all the examined samples contain microfossils with silica skeleton and a small amount of diagenetically redistributed silica as cement. Biogenic and diagenetic fraction of the Si may cause the extremely high Si content of a few carbonate–rich semicouplets and the above mentioned value of the Si–Ti linear regression.

Aluminium and titanium concentrations are generally used to correct for the terrestrial influences in marine sediments while these elements are regarded as immobile under conditions of sedimentary and diagenetic environments (MURRAY et al. 1991, MURRAY & LEINEN 1996, CULLERS 2000). In $CaCO_3$–rich biogenic sediments, however, a part of the aluminium may be connected to the biogenic fraction (MURRAY et al. 1993, MURRAY & LEINEN 1996). This biogenic effect on the aluminium distribution seems to be reasonable as the linear regression value between the Al and Ti ($r=0.414$, $n=25$) suggests. Also in the case of samples derived from the Komló Calcareous Marl Formation, using the aluminium normalisation and the Al/(Al+Fe+Mn) ratio proposed by BELLANCA et al. (1996) seem to be unrealistic. In contrast of the Al, bioaffinity–related distortion of the Ti distribution (in normal marine environment) is unknown. Therefore, Ti seems to be a good tool to represent the terrigenous component of the samples.

Calcite content of the samples is the main factor controlling the concentrations of calcium. This is indicated by the average CaO values of the carbonate–rich and carbonate–poor semicouplets (39.20% and 23.24%, respectively) and by the significantly negative Ca–Ti linear regression value ($r=-0.835$, $n=25$).

In sedimentary rocks, concentration of potassium is mainly controlled by the amount of phyllosilicates. This idea is supported by the excellent correlation of the K–Ti ($r=0.956$, $n=25$).

Concentrations of iron show significant positive correlations to the terrigenous elements such as Ti ($r=0.952$, $n=25$) and K ($r=0.935$, $n=25$) showing detrital control on this element. However, there are samples characterised by significant Ti–normalised enrichment of the Fe relative to the PAAS (Table V.). This suggests another (probably seawater) source of the Fe in addition to the lattice–bound aluminosilicate contribution to the sediment (MURRAY & LEINEN 1993). According to the macroscopic and microscopic observations, the excess amount of Fe is bound to pyrite, limonite and hematite (these latter are mostly pseudomorphs

after iron sulfide) what may indicate role of diagenetic redistribution of the reactive iron (BERNER 1981, MORSE et al. 1987, HUERTA–DIAZ & MORSE 1992, LUTHER & MORSE 1998, LYONS et al. 1998).

Trace elements in sediments that accumulate on the seafloor have two sources: detrital clastic matter and seawater (KUMAR et al. 1996). The seawater–derived fraction also has two components: a portion that is incorporated into the marine organisms and a component that is scavenged from the dissolved load of seawater by organic and inorganic particles settling through the water column. Relation of the trace elements to an immobile detrital–related element (such that in our case the Ti) defined for PAAS (TAYLOR & MCLENNAN 1985), as stated above, seems to be an available tool to estimate excess amount (over detrital) of the trace elements. Enrichment factors of the phosphorous, manganese, vanadium, chromium, nickel, zinc and copper (Table V.) show significant contribution of the seawater–derived fraction to the total concentrations.

Phosphorous (with strontium and barium) in marine sediment is commonly affiliated with biogenic phases (FROELICH et al. 1982, FISHER et al. 1991, PINGITORE et al. 1992, MURRAY & LEINEN 1993) and as such is commonly enriched in sediment deposited beneath productive surface waters (FROELICH et al. 1982, BISHOP 1988, FISHER et al. 1991, INGALL & CLARK 1998, MATTENBERGER et al. 1998). P correlates well with the Ca ($r=0.870$). According to its Ti–normalised enrichment factors relative to the PAAS (Table V.) only a small part of the P may be explained by detrital terrigenous phases (presence of apatite and adsorption of the P onto clay minerals). A significant portion seems to be related to disseminated biogene apatite–group phases which originally incorporated into the siliceous and carbonate skeleton of organisms (BISHOP 1988). The transporting agents (opal and calcite or aragonite) partially degraded on the seafloor during early diagenesis leaving behind the P record as a dissolution residue. Two orders of magnitude Ti–normalised enrichment of the P relative to the PAAS seems to indicate enhanced productivity during deposition of the carbonate–rich beds.

The high sensitivity of manganese to environmental redox conditions is well known (DROMGOOLE & WALTER 1990; GOBEIL et al. 1997). In hemipelagic sediments subjected to a transition from suboxic (or anoxic) to oxic conditions, low Eh conditions can lead to a Mn enrichment in the pore water and the subsequent diffusion of dissolved Mn may concentrate this element in the solid phase, just above or below the redox boundary (JACOBS et al. 1985, LANDING & BRULAND 1987). DICKENS & OWEN (1994) have suggested that the redox–sensitive Mn oxi-hydroxide particulates dissolve upon entering an oxygen minimum zone. The resulting Mn^{2+} is subsequently redirected by advective and/or diffusive processes eventually to precipitate in more oxygenated environments. The record of Mn may reflect migration of the metal from the moderately oxygenated parts of the sediment and its diagenetic enrichment in the more oxygenated parts during early diagenesis. Thus the fluctuation of Mn values may be interpreted as an indicator of rhythmic

changes in sedimentary redox conditions. The Ti–normalised enrichment factors of Mn are fluctuate from below unity to about 19 (Table V.). Maximum enrichment is related to the carbonate–rich layers, relative impoverishment appears in the case of the carbonate–poor ones what can be explained by the above–mentioned diagenetic redistribution model.

Vanadium fluctuates through the section exhibiting low values for carbonate–rich layers (average value is 102 ppm) and slightly higher values in the carbonate–poor intervals (average value is 137 ppm). V shows slight positive correlation with the Ti ($r= 0.707$, $n= 16$) and in the case of many samples significant enrichment relative to the PAAS (Table V.) suggesting that the affiliation with the aluminosilicates is not an exclusive control on the V concentration in the studied section. Vanadium solubility in natural waters, its precipitation from seawater and addition to the sediments are controlled by redox conditions and by adsorption and complexation processes. Dissolved vanadium may be strongly bound to metallo–organic complexes or adsorbed on biogenic particles (NORMAN & DE DECKKER 1990; BREIT & WANTY 1991). Adsorption and complexation of V are enhanced in anoxic environments where V is present as reduced V (IV) species. During post–depositional and diagentic alteration of sediments, V can be mobilised from degrading biogenic particles under oxic conditions, while it is less mobile in dysoxic and anoxic sediments.

Correlation between Ni and Ti is good ($r=0.870$, $n=19$). Many workers give account of lower redox–sensitivity of Ni relative to the other elements, above all to vanadium (SHAW et al. 1990, ODERMATT & CURIALE 1991, HUERTA–DIAZ & MORSE 1992, PIPER 1994). These features suggest that the main source of Ni is the terrigenous fraction, however some degree of diagenetically–controlled enrichment, cannot to be excluded.

The data indicate that the zinc and copper concentration (up to 102 ppm and 30 ppm, respectively) is about 1.5 to 7 times the amount can be explained from a pure aluminosilicate source (Table V.). The correlation between the Zn and the Ti is excellent ($r=0.920$, $n=25$), however, Cu show less good correlation with the main detritus–related element ($r=0.769$, $n=22$). Excess concentrations of these chalcophile elements may also be in sulfides. More likely, some of the excess amount of them was primarily associated with organic fraction, either as metal–organic complexes or adsorbed on organic coatings in particulate organic matter (BALISTRIERI et al. 1981, BRULAND 1983). It is noteworthy that organic matter derived from plankton has an average concentrations of Zn of 110 ppm (DEAN et al. 1997).

The studied rock samples are characterised by significantly higher carbonate content than that of PAAS. The observed enrichments suggest that fluctuations of the trace elements cannot be explained merely by dilution effects, because the examined trace elements show affinity to the incorporation in sulfides and aluminosilicates or adsorption on their surfaces. If dilution had controlled the trace element distribution, a significant impoverishment for most of the measured elements would have been observed relative to the PAAS. In the case of the manganese,

redox–controlled diagenetic redistribution (and eventually incorporation into the lattice of calcite) seems to be a reliable explanation.The presented trace elements suggest occurrence of fluctuations in the redox state of the depositional environment. It seems probable that during well–oxygenated periods of sedimentation (during deposition of carbonate–rich semicouplets) organo–metal complexes oxydised then migrated in the sediment and in the seawater. During periods characterised by less oxygenated and, probably, dysoxic seafloor (deposition of carbonate–poor semicouplets) these metals and organo–metal complexes could remain in reduced, consequently less mobile state (NORMAN & DE DECKKER 1990, SHAW et al. 1990, MARCHITTO et al. 1998).

a ARID-STATE

high δ^{18}O, high salinity, high δ^{13}C

anti-estuarine circulation *evaporation*

low rate of weathering

calcareous sediments

b HUMID-STATE

low δ^{18}O, low salinity low δ^{13}C

intense weathering

estuarine circulation

argillaceous sediments
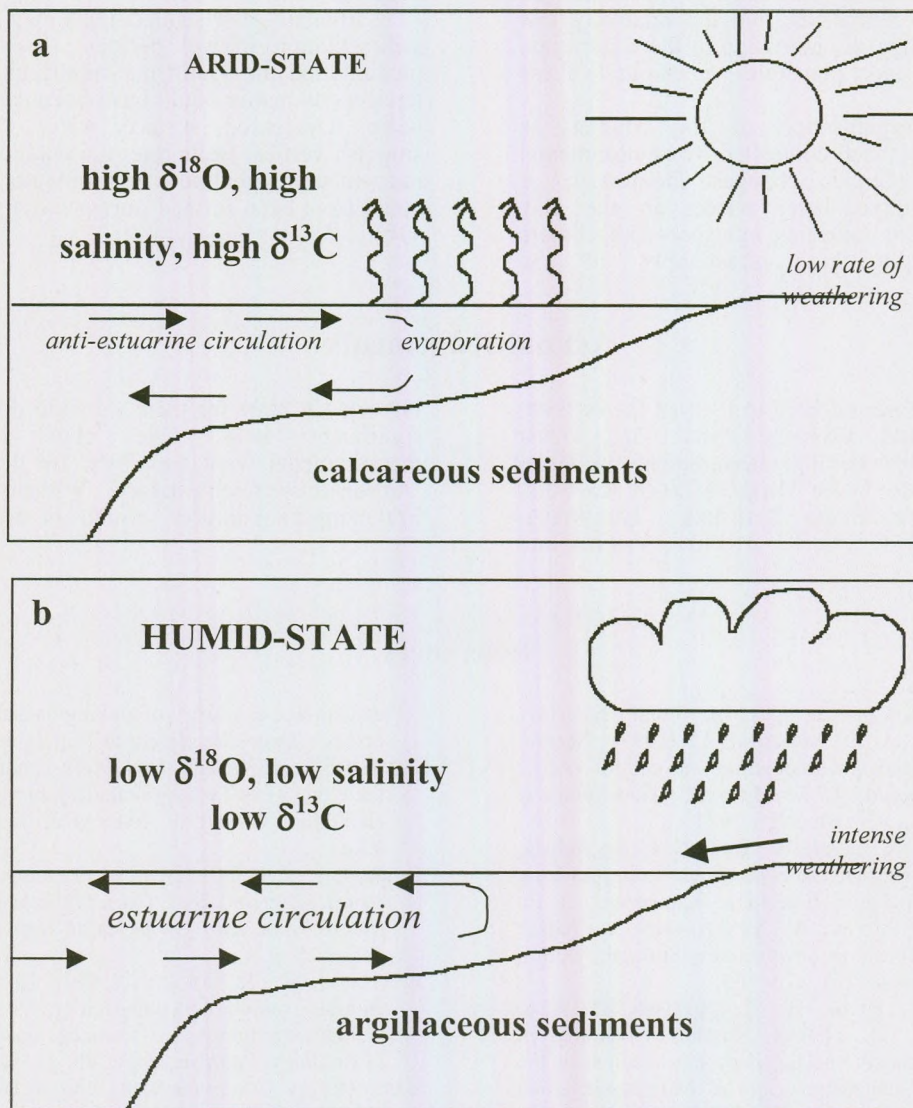
Fig. 11. Schematic view of the palaeoenvironmental scenario during a: arid episodes and b: humid episodes

Depositional model

Rhythmic bedding of the Komló Calcareous Marl Formation seems to be formed by primary processes. Diagenesis has just overprinted the primary signal due to the lack of pervasive dissolution features and the oxygen isotope data. Redeposition of the fine carbonate mud from the neighbouring shelf by nepheloid plumes and/or by bottom currents as autocyclic processes cannot be excluded from the rhythmicity–forming driving forces according to the presence of abundant shelf–derived bioclasts in microfacies of some carbonate rich samples and the maxima of the kaolinite abundance that closely relate to these samples.

During deposition of the carbonate–rich semicouplets, depositional environment seems to be characterised by (i) well oxygenation of the seafloor, (ii) relatively 'cooler' and/or 'more saline' surface water, with (iii) enhanced productivity according to (i) the pervasive bioturbation, (ii) the relatively high δ^{18}O values, (iii) the positive excursions of the enrichment of phosphorous, the high radiolarian abundance and the relatively high δ^{13}C values.

These factors seem to be controlled by intensive circulation of the water mass of the basin.

Contrarily, properties of the carbonate–poor semicouplets show (i) relatively poor oxygenation of the seafloor, (ii) relatively 'warmer' and/or 'less saline' surface water with (iii) normal or depressed productivity suggested by (i) the enrichment properties of the redox–sensitive trace elements, (ii) the relatively low $\delta^{18}O$ values, (iii) the negative excursions of the enrichment of phosphorous, the low radiolarian abundance and the relatively low $\delta^{13}C$ values. Sluggish circulation of the water mass seems to be the most plausible explanation of these phenomena.

Rhythmic organisation of the couplets is believed to have been controlled by environmental and probably climatic changes. Dominance of illite/smectite mixed–layer phases in the clay mineral spectrum indicates monsoon–like climate characterised by high seasonality in the precipitation during deposition of the Komló Calcareous Marl Formation. During dry periods, streams could carry low amount of terrigenous matter. Seawater salinity could have been increased, which could form intensive anti–estuarine circulation and well bottom oxygenation with abundant nutrient supply and enhanced productivity. Carbonate–rich semicouplets seem to be formed by this palaeoenvironmental conditions (Fig. 11a).

Carbonate–poor semicouplets may represent the sedimentation in wet periods. Due to abundant precipitation and continental runoff, high amount of terrigenous matter could have been carried into the basin. Decreased surface water salinity with sluggish vertical (estuarine–) circulation, decreased nutrient supply and poor bottom water oxygenation could have been formed during these periods (Fig. 11b).

Acknowledgements

References

ABOUCHAMI, W., GOLDSTEIN, S. L., GALER, S. J. G., EISENHAUER, A. & MANGINI, A. (1997): Secular changes of lead and neodymium in central Pacific seawater recorded by a Fe–Mn crust. – *Geochimica et Cosmochimica Acta* 61, 3957–3974.

ARTHUR, M. A. & DEAN, W. E. (1991): An holistic geochemical approach to cyclomania: examples from Cretaceous pelagic limestone sequences. – In: EINSELE, G., RICKEN, W. & SEILACHER, A. (eds.): *Cycles and Events in Stratigraphy.* Springer, Berlin, Heidelberg, New York, 126–166.

ARTHUR, M. A., DEAN, W. E., BOTTJER, D. J. & SCHOLLE, P. A. (1984): Rhythmic bedding in Mesozoic–Cenozoic pelagic carbonate sequences: the primary and diagenetic origin of Milankovitch–like cycles. – In: BERGER, A., IMBRIE, J., HAYS, J., KUKLA, G. & SALTZMAN, B. (eds.): *Milankovitch and climate. NATO series* C126, I. Reidel, Dordrecht, 191–222.

ARTHUR, M. A., BOTTJER, D. J., DEAN, W. E., FISCHER, A. G., HATTIN, D. E., KAUFFMAN, E. G., PRATT, L. M. & SCHOLLE, P. A. = ROCC Group (1986): Rhythmic bedding in Upper Cretaceous pelagic carbonate sequences: Varying sedimentary response to climatic forcing. – *Geology* 14, 153–156.

BALÁZS, E., CSEREPES-MESZÉNA, B., NUSSZER, A., SZILI, GY & GYÉMÁNT, P. (1986): An attempt to correlate the methamorphic formations of the Great Hungarian Plain and the Transylvanian Central Mountains (Munţii Apuseni). – *Acta Geologica Hungarica* 29, 317–320.

BALISTRIERI, L., BREWER, P. G. & MURRAY, J. W. (1981): Scavenging residence times of trace metals and surface chemistry of sinking particles in the deep ocean. – *Deep–Sea Research* 28, 101–121

BARRERA, E. & KELLER, G. (1994): Productivity across the Cretaceous/Tertiary boundary in high latitudes. – *Geological Society of America Bulletin* 106, 1254–1266.

BARRON, E. J. (1986): Physical oceanography: a status report. – In: HSÜ, K. J. (ed.): *Mesozoic and Cenozoic oceans. American Geophysical Union Geodynamic Series* 15, 1–9.

BARTOLINI, A., & GUEX, J. (1999): Middle and Late Jurassic radiolarian paleoecology versus carbon–isotope stratigraphy – *Palaeogeography, Palaeoclimatology, Palaeoecology* 145, 43–60.

BARTOLINI, A., BAUMGARTNER, P. O. & HUNZIKER, J. C. (1996): Middle and Late Jurassic carbon stable–isotope stratigraphy and radiolarite sedimentation of the Umbria–Marche Basin (Central Italy). – *Eclogae Geologicae Helvetiae* 89/2, 811–844.

BARTOLINI, A., MORETTINI, E., O'DOGHERTY, L., SANDOVAL, J., BAUMGARTNER, P O. & HUNZIKER, J. C. (1997): Carixian–Bajocian carbon isotope stratigraphy of the Umbria–Marche (Central Italy) and Subbetic (Spain) areas. – In: *European Union of Geosciences, Strasbourg, France 23–27 March 1997 Abstract Supplement No. 1 Terra Nova* 9, 403 p.

BELLANCA, A., DI STEFANO, P. & NERI, R. (1995): Sedimentology and isotope geochemistry of Carnian deep–water marl/limestone deposits from the Sicani Mountains, Sicily: Environmental implications and evidence for planktonic source of lime mud. – *Palaeogeography, Palaeoclimatology, Palaeoecology* 114, 111–129.

BELLANCA, A., CLAPS, M., ERBA, E., MASETTI, D., NERI, R., PREMOLI SILVA, I. & VENEZIA, F. (1996): Orbitally induced limestone/marlstone rhythms in the Albian–Cenomanian Cismon section (Venetian region, northern Italy): sedimentology, calcareous and siliceous plankton distribution, elemental and isotope geochemistry. – *Palaeogeography, Palaeo–climatology, Palaeoecology* 126, 227–260.

BERGER, A. & VINCENT, E. (1986): Deep–sea carbonates: Reading the carbon isotope signal. – *Geologische Rundschau* 75/1, 249–269.

BERGER, A., IMBRIE, J., HAYS, J., KUKLA, G. & SALTZMAN, B. (eds.) (1984): *Milankovitch and Climate. NATO series* C126, I, II. – Reidel, Dordrecht, 895 p.

BERNER, R. A. (1981): A new geochemical classification of sedimentary environments. – *Journal of Sedimentary Petrology* 51, 359–365.

BHATIA, M. R. (1983): Plate tetonics and geochemical composition of sandstones. – *Journal of Geology* 91/6, 611–627

BICKERT, T., PÄTZOLD, J., SAMTLEBEN, C. & MUNNECKE, A. (1997): Paleoenvironmental changes in the Silurian indicated by stable isotopes in brachiopod shells from Gotland, Sweden. – *Geochimica et Cosmochimica Acta* 61/13, 2717–2730.

BILL, M., BAUMGARTNER, P. O., HUNZIKER, J. C. & SHARP, Z. D. (1995): Carbon isotope stratigraphy of the Liesberg Beds Member (Oxfordian, Swiss Jura) using echinoids and crinoids – *Eclogae Geologicae Helvetiae* 88/2, 817–832.

BISCAYE, P. E. (1965): Mineralogy and sedimentation of recent deep–sea clay in the Atlantic Ocean and adjacent seas and oceans. – *Geological Society of America Bulletin* 76, 803–832.

BISHOP, J. K. B. (1988): The barite–opal–organic carbon association in oceanic particulate matter. – *Nature* 332, 341–343.

BLEAHU, M. (1976): Structural position of the Apuseni Mountains in the Alpine system. – *Rev. Roum. Géol. Géophys. Géogr., Ser Géol.* 20, 7–19.

BORBÉLY–KISS, I., KOLTAY, E., LÁSZLÓ, S., SZABÓ, GY. & ZOLNAI, L. (1985): Experimental and theoretical calibration of a PIXE setup for K and L–rays. – *Nuclear Instruments and Methods in Physics Research* B12, 496–504.

BOTTJER, D. J., ARTHUR, M. A., DEAN, W E., HATTIN, D. E. & SAVRDA, C. E. (1986): Rhythmic bedding produced in Cretaceous pelagic carbonate environments: sensitive recorders of climatic cycles. – *Paleoceanography* 1, 467–481.

BREIT, G. N. & WANTY, R. B. (1991): Vanadium accumulation in carbonaceous rocks: A review of geochemical controls during deposition and diagenesis. – *Chemical Geology* 91, 83–97.

BRULAND, K. W. (1983): Trace elements in seawater. – In: RILEY, J. P. & CHESTER, R. (eds.): *Chemical Oceanography* 157–220, Academic Press, New York.

BUCEFALO PALLIANI, R., CIRILLI, S. & MATTIOLI, E. (1998): Phytoplankton response and geochemical evidence of the lower Toarcian relative sea level rise in the Umbria–Marche basin (Central Italy). – *Palaeogeography, Palaeoclimatology, Palaeoecology* 142, 33–50.

CAPLAN, M. L., & BUSTIN, R. M. (1999): Devonian–Carboniferous Hangenberg mass extinction event, widespread organic–rich mudrock and anoxia: causes and consequences. – *Palaeogeography, Palaeoclimatology, Palaeoecology* 148, 187–207.

ÇELIK, M., KARAKAYA, N. & TEMEL, A. (1999): Clay minerals in hydrothermally altered volcanic rocks, Eastern Pontides, Turkey. – *Clays and Clay Minerals*, 47/6, 708–717.

CHAMLEY, H. (1967): Possibilities of utilisation of the crystallinity of a clay mineral (illite) as climatic evidence in Recent sediments (In French with English abstract). – *C. R. Acad. Sci.* 265, 184–187

CHAMLEY, H. (1989): *Clay Sedimentology*. – Springer, Berlin, Heidelberg, New York, 623 p.

CHAMLEY, H. & DEBRABANT, P (1984): Paleoenvironmental history of the North Atlantic region from mineralogical and geochemical data. – *Sedimentary Geology*, 40, 151–167

CHANDLER, M. A., RIND, D. & RUEDY, R. (1992): Pangean climate during the Early Jurassic: GCM simulations and the sedimentary record of paleoclimate. – *Geological Society of America Bulletin* 104, 543–559.

COLACICCHI, R., BARTOLINI, A. & BAUMGARTNER, P. O. (2000): Siliceous sedimentation in the Mediterranean Jurassic caused by volcanism, greenhouse climate and eutrophication – *GeoResearh Forum (5th Jurassic Symposium, Vancouver)* 6, 417–426.

COOK, H. E. & EGBERT, R. M. (1983): Diagenesis of deep–sea carbonates. – In: LARSEN, G. & CHILINGAR, G. V (eds.): *Diagenesis in Sediments and Sedimentary Rocks 2. Developments in Sedimentology* 25B, 213–288. Elsevier, Amsterdam.

CORNIDES, I., CSÁSZÁR, G., HAAS, J. & JOCHA–EDELÉNYI, E. (1979): Oxygen isotopic temperature measurements from Mesozoic formations of Transdanubia (In Hungarian). – *Földtani Közlöny* 109, 101–110.

CULLERS, R. L. (2000): The geochemistry of shales, siltstones and sandstones of Pennsylvanian–Permian age, Colorado, USA. implications for provenance and metamorphic studies. – *Lithos* 51, 181–203.

CSÁSZÁR, G. (ed.) (1997): *Basic lithostratigraphic units of Hungary (Magyarország litosztratigráfiai alapegységei, In Hungarian)* – MÁFI, Budapest.

DEAN, W. E., GARDNER, J. V & PIPER, D. Z. (1997): Inorganic geochemical indicators of glacial–interglacial changes in productivity and anoxia on the California continental margin. – *Geochimica et Cosmochimica Acta* 61/21, 4507–4518.

DE BOER, P. L. (1983): Aspects of Middle Cretaceous pelagic sedimentation in S Europe. – *Geologica Ultraiectana* 31, 112.

DE BOER, P. L. (1991): Pelagic black shale–carbonate rhythms: Orbital forcing and oceanographic response. – In: EINSELE, G., RICKEN, W & SEILACHER, A. (eds.): *Cycles and Events in Stratigraphy*. Springer, Berlin, Heidelberg, New York, 63–78.

DE BOER, P L. & SMITH, D. G. (1994): Orbital forcing and cyclic sequences. – In: DE BOER, P. L. & SMITH, D. G. (eds.): *Orbital Forcing and Cyclic Sequences. IAS Special Publications* 19, 1–14.

DICKENS, G. R. & OWEN, R. M. (1994): Late Miocene–Early Pliocene manganese redirection in the central Indian Ocean. Expansion of the intermediate water oxygen minimum zone. – *Paleoceanography* 9, 161–181.

DOWDY, S. & WEARDEN, S. (1983): *Statistics for Research*. – John Wiley & Sons, Chichester, 537 p.

DROMGOOLE, E. L. & WALTER, L. M. (1990): Iron and manganese incorporation into calcite: Effects of growth kinetics, temperature and solution chemistry. – *Chemical Geology* 81, 311–336.

DUFF, P M., HALLAM, A. & WALTON, E. K. (eds.) (1967): *Cyclic Sedimentation. Developments in Sedimentology* 10. – Elsevier, Amsterdam, 280 p.

DUNKL, I. (1992): Fission track evidences on thermal history and uplift of the Eastern Mecsek Mts., Hungary – Preliminary results (In Hungarian with English abstract). – *Általános Földtani Szemle* 26, 163–168.

DYMOND, J., SUESS, E. & LYLE, M. (1992): Barium in deep–sea sediment: A geochemical proxy for paleoproductivity. – *Paleoceanography* 7, 163–181.

EGGER, H., BICHLER, M., DRAXLER, I., HOMAYOUN, M., HUBER, H. J., KIRCHNER, E. C., KLEIN, P. & SURENIAN, R. (1997): Mudturbidites, Black Shales and Bentonites from Paleocene/Eocene Boundary. The Anthering Formation of the Rhenodanubian Flysch (Austria). – *Jahrbuch der Geologische Bundesanstalt*, 140/1, 29–45.

EINSELE, G. & RICKEN, W. (1991): Limestone–marl alternartion – an overview. – In: EINSELE, G., RICKEN, W. & SEILACHER, A. (eds.): *Cycles and Events in Stratigraphy.* Springer, Berlin, Heidelberg, New York, 23–47

EINSELE, G. & SEILACHER, A. (eds.) (1982): *Cyclic and Event Stratification.* – Springer, Berlin, Heidelberg, New York, 536 p.

EINSELE, G., RICKEN, W. & SEILACHER, A. (1991): Cycles and Events in Stratigraphy – Basic concepts and terms. – In: EINSELE, G., RICKEN, W. & SEILACHER, A. (eds.): *Cycles and Events in Stratigraphy.* Springer, Berlin, Heidelberg, New York, 3–19.

ELDERFIELD, H. (1990): Tracers of ocean paleoproductivity and paleochemistry· An introduction. – *Paleoceanography* 5, 711–717.

EMRICH, K., EHHALT, D. H. & VOGEL, J. C. (1970): Carbon isotope fractionation during the precipitation of calcium carbonate. – *Earth and Planetary Science Letter* 8, 363–371.

ERBA, E. & PREMOLI SILVA, I. (1994): Orbitally driven cycles in trace–fossil distribution from the Piobbico core (late Albian, central Italy). – *Special Publications of International Association of Sedimentologists* 19, 211–225.

FAGEL, N., ANDRÉ, L. & DEBRABANT, P (1997): Multiple seawater–derived geochemical signatures in Indian oceanic pelagic clays. – *Geochimica et Cosmochimica Acta* 61, 989–1008.

FILIPPELLI, G. M. & DELANEY, M. L. (1996): Phosphorus geochemistry of equatorial Pacific sediments. – *Geochimica et Cosmochimica Acta* 60, 1479–1495.

FISCHER, A. G., DE BOER, P. L. & PREMOLI SILVA, I. (1990): Cyclostratigraphy. – In: GINSBURG, R. N. & BEAUDOIN, B. (eds.): *Cretaceous Resources, Events and Rhythms – Background and Plans for Research.* Kluwer, Dordrecht, 139–172.

FISHER, N. S., GUILLARD. R. R. L. & BANKSTON D. C. (1991): The accumulation of barium in marine phytoplankton grown in culture. – *Journal of Marine Research* 49, 339–354.

FOGARASI, A. (1995): Cretaceous cyclostratigraphy of Gerecse Mts. Preliminary results (In Hungarian, with English abstract). – *Általános Földtani Szemle* 27, 43–58.

FORGÓ L., MOLDVAY L., STEFANOVITS P. & WEIN Gy. (1966): *Explanation to Geological Map of Hungary, Series 1.200,000, L–34–XIII. Pécs* (In Hungarian). – MÁFI, Budapest, 196 p.

FÖLLMI, K. B., WEISSERT, H., BISPING, M. & FUNK, H. P. (1994): Phosphogenesis, carbon–isotope stratigraphy, and carbonate platform evolution along the Lower Cretaceous Northern Tethyan margin. – *Geological Society of America Bulletin* 106, 729–746.

FRANCK, S., KOSSACKI, K. & BOUNAMA, C. (1999): Modelling the global carbon cycle for the past and future evolution of the earth system. – *Chemical Geology* 159, 305–317.

FRIEDMAN, I. & O'NEIL, J. R. (1977): Compilation of stable isotope fractionation factors of geochemical interest. – In: *Data of Geochemistry 6th . Geological Survey Professional Paper* 440–KK.

FROELICH, P. N., BENDER, M. L., LUEDTKE, N. A. & HEATH, G. R. (1982): The marine phosphorous cycle. – *American Journal of Science* 282, 474–511.

GIBSON, T G., BYBELL, L. M. & MASON, D. B. (2000): Stratigraphic and climatic implications of clay mineral changes around the Paleocene/Eocene boundary of the northeastern US margin. – *Sedimentary Geology* 134, 65–92.

GOBEIL, C., MACDONALD, R.W & SUNDBY, B. (1997): Diagenetic separation of cadmium and manganese in suboxic continental margin sediments. – *Geochimica et Cosmochimica Acta* 61/21, 4647–4654.

GROSSMAN, E. L., ZHANG, C. & YANCEY, T. E. (1991): Stable–isotope stratigraphy of brachiopods from Pennsylvanian shales in Texas. – *Geological Society of America Bulletin* 103, 953–965.

GROSSMAN, E. L., MII, H. & YANCEY, T E. (1993): Stable–isotopes in Late Pennsylvanian brachiopods from the United States: Implications for Carboniferous paleoceanography. – *Geological Society of America Bulletin* 105, 1284–1296.

GROW, J. A. MATTICK, R. E., BÉRCZY–MAKK, A., PÉRÓ, CS., HAJDÚ, D., POGÁCSÁS, GY., VÁRNAI, P. & VARGA, E. (1986): Structure of the Békés Basin inferred from seismic reflection, well and gravity data. – In: TELEKI, P. G. (ed.): *Basin Analysis in Petroleum Exploration,* Kluwer, Dordrecht, 1–38.

GYGI, R. A. & PERSOZ, F. (1986): Mineralostratigraphy, litho– and biostratigraphy combined in correlation of the Oxfordian (Late Jurassic) formations of the Swiss Jura range. – *Eclogae Geologicae Helvetiae*, 79/2, 385–454.

HAAS, J. (1982): Facies analysis of the cyclic Dachstein Limestone Formation (Upper Triassic) in the Bakony Mountains. – *Facies* 6, 75–84.

HALLAM, A. (1964): Origin of the limestone–marl rhythm in the Blue Lias of England: a composite theory. – *Journal of Geology* 72, 157–169.

HALLAM, A. (1984): Continental humid and arid zones during the Jurassic and Cretaceous. – *Palaeogeography, Palaeoclimatology, Palaeoecology* 47, 195–223.

HALLAM, A., GROSE, J. A. & RUFFELL, A. H. (1991): Palaeoclimatic significance of changes in clay mineralogy across the Jurassic–Cretaceous boundary in England and France. – *Palaeogeography, Palaeo–climatology, Palaeoecology* 81, 173–187.

HARNOIS, L. (1988): The CIW index: a new chemical index of weathering. – *Sedimentary Geology* 55, 319–322.

HOLLANDER, D. J., MCKENZIE, J. A. & HSÜ, K. J. (1993): Carbon isotope evidence for unusual plankton blooms and fluctuations of surface water CO_2 in 'Strangelove Ocean' after terminal Cretaceous event. – *Palaeogeography, Palaeoclimatology, Palaeoecology* 104, 229–237.

HOWER, J. (1981): Shale diagenesis. – In: LONGSTAFFE, F. J. (ed.): *Clays and the Resource Geologist.*

Mineralogical Association of Canada, Short Course Handbook 7, 60–80.

HOWER, J., ESLINGER, E. V., HOWER, M. E. & PERRY, E. A. (1976): Mechanism of burial metamorphism of argillaceous sediments: 1. Mineralogical and chemical evidence. – *Geological Society of America Bulletin* 87, 725–737.

HUANG, W. L. (1993): The formation of illitic clays from kaolinite in KOH solution from 225°C to 350°C. – *Clays and Clay Minerals* 41/6, 645–654.

HUERTA–DIAZ, M. A. & MORSE, J. W. (1992): Pyritization of trace metals in anoxic marine sediments. – *Geochimica et Cosmochimica Acta* 56, 2681–2702.

HUISMAN, D. J., KLAVER, G. T., VELDKAMP, A. & VAN OS, B. J. H. (2000): Geochemical compositional changes at the Pliocene–Pleistocene transition in fluviodeltaic deposits in the Tegelen–Reuver area (southeastern Netherlands). – *International Journal of Earth Sciences* 89, 154–169.

IANOVICI, V., BORCOS, M., BLEAHU, M., PATRULIUS, D., LUPU, M., DIMITRESCU, R. & SAVU, H. (1976): *Geology of Transylvanian Central Mountains (Munţii Apuseni).* (In Rumanian) – Edit. Acad. R. S. R. Bucureşti, 631 p.

INGALL, E. & CLARK, L. (1998): Redox dependent phosphorous cycling: Microbial and abiotic processes. – *Goldschmidt Conference for Geochemistry, Toulouse 1998, Abstract Vol.* 677–678.

JACOBS, L., EMERSON, S. & SKEI, J. (1985): Partitioning and transport of metals across the O_2/H_2S interface in a permanently anoxic basin: Framvaren Fjord, Norway. – *Geochimica et Cosmochimica Acta* 49, 1433–1444.

JACOBSEN, S. B. & KAUFMAN, A. J. (1999): The Sr, C and O isotopic evolution of Neoproterozoic seawater. – *Chemical Geology* 161, 37–57

JENKYNS, H. C. (1996): Relative sea–level change and carbon isotopes: data from the Upper Jurassic (Oxfordian) of Central and Southern Europe – *Terra Nova* 8/1, 75–85.

JENKYNS, H. C. & CLAYTON C. J. (1986): Black shales and carbon isotopes in pelagic sediments from the Tethyan Lower Jurassic. – *Sedimentology* 33, 87–106.

JENKYNS, H. C., GALE, A. S. & CORFIELD, R. M. (1994): Carbon– and oxygen–isotope stratigraphy of the English Chalk and Italian Scaglia and its paleoclimatic significance. – *Geological Magazine* 131, 1–34.

JOACHIMSKI, M. M., PANCOST, R. D., FREEMAN, K. H. & OSTERTAG–HENNING, C. (1998): Compound–specific isotope analysis across the Frasnian–Famennian boundary. – *Goldschmidt Conference for Geochemistry, Toulouse 1998, Abstract Vol.* 719–720.

JOHANSSON, S. A. E. & CAMPBELL, J. L. (1988): PIXE: A Novel Technique for Elemental Analysis. – John Wiley & Sons, Chichester. 632 p.

KAUFFMAN, E. G. (1988): Concepts and methods of high–resolution event stratigraphy. – *Annual Reviews of Earth and Planetary Sciences* 16, 605–654.

KILLINGEY, J. S. (1983): Effects of diagenetic recrystallization on $^{18}O/^{16}O$ values of deep–sea sediments. – *Nature* 301, 594–597.

KUMAR, N., ANDERSON, R. F & BISCAYE, P E. (1996): Remineralization of particulate authigenic trace metals in the Middle Atlantic Bight: Implications for proxies of export production. – *Geochimica et Cosmochimica Acta* 60, 3383–3397.

KUMP, L. R. (1989): Alternative modeling approaches to the geochemical cycles of carbon, sulfur, and strontium isotopes. – *American Journal of Science* 289/4, 390–410.

KUMP, L. R. (1991): Interpreting carbon–isotope excursions: Strangelove oceans. – *Geology* 19, 299–302.

KUMP, L. R. & ARTHUR, M. A. (1999): Interpreting carbon–isotope excursions: carbonates and organic matter. – *Chemical Geology* 161, 181–198.

KUTZBACH, J. E. & GALLIMORE, R. G. (1989): Pangean climates: megamonsoons of the megacontinent. – *Journal of Geophysical Research* 94, 3341–3357.

LAFERRIERE, A. P (1992): Regional isotopic variations in the Fort Hays Member of the Niobrara Formation, United States Western Interior: Primary signals and diagenetic overprinting in a Cretaceous pelagic rhythmite. – *Geological Society of America Bulletin* 104, 980–992.

LANDIG, W. M. & BRULAND, K. W. (1987): The contrasting biogeochemistry of iron and manganese in the Pacific Ocean. – *Geochimica et Cosmochimica Acta* 51, 29–43.

LANDIS, G. P (1983): Harding Iceland Spar: A new $\delta^{18}O$–$\delta^{13}C$ carbonate standard for hydrothermal minerals. – *Chemical Geology (Isotope Geosciemce Section)* 1, 91–94.

LASAGA, A. C. (1989): A new approach to isotopic modeling of the variation of atmospheric oxygen through the Phanerozoic. – *American Journal of Science* 289/4, 411–435.

LONG, D. G. F. (1993): Oxygen and carbon isotopes and event stratigraphy near the Ordovician–Silurian boundary, Anticosti Island, Quebec. – *Palaeogeography, Palaeoclimatology, Palaeoecology* 104, 49–59.

LUTHER III, G. W & MORSE, J. W. (1998): Chemical influences on trace metal–sulphide interactions in anoxic sediments. – In: *Goldschmidt Conference for Geochemistry, Toulouse 1998, Abstract Vol.* 925–926.

LYLE, M., MURRAY, D. W., FINNEY, B. P., DYMOND, J., ROBBINS, J. M. & BROOKSFORCE, K. (1988): The record of Late Pleistocene biogenic sedimentation in the eastern tropical Pacific Ocean. – *Paleoceanography* 3, 39–59.

LYONS, T W., WERNE, J. P., HOLLANDER, D. J., MURRAY, R. W., PEARSON, D. G. & PETERSON, L. C. (1998): Biogeochemical pathways in Holocene and latest Pleistocene sediments of the anoxic Cariaco Basin: Linkages to palaeoceanographic and palaeoclimatic variability – *Goldschmidt Conference for Geochemistry, Toulouse 1998, Abstract Vol.* 931–932.

MAGARITZ, M. & HOLSER, W T (1990): Carbon isotope shifts in Pennsylvanian seas. – *American Journal of Science* 290, 977–994.

MARCHITTO, T M., CURRY, W B. & OPPO, D. W (1998): Benthic foraminiferal Zn/Ca, a new tracer of deep water palaeocirculation? – In: *Goldschmidt Conference for Geochemistry, Toulouse 1998, Abstract Volume* 945–946.

MARSHALL, J. D. & BRENCHLEY, P J. (1998): Oceanic and atmospheric changes at the end of the Ordovician: geochemical enigmas or the end of a beautiful hypothesis? – In: *Goldschmidt Conference for Geochemistry, Toulouse 1998, Abstract Volume* 951–952.

MARTINEZ, P., BERTRAND, P., SHIMMIELD, G. B., COCHRANE, K., JORISSEN, F J., FOSTER, J. & DIGNAN, M. (1999): Upwelling intensity and ocean productivity changes off Cape Blanc (northwest Africa) during the last 70,000 years: geochemical and micropalaeontological evidence. – *Marine Geology* 158, 57–74.

MATTENBERGER, CH., WÜEST, A., STURM, M., GOUDSMIT, G. & BARBIERI, A. (1998): Redox– and mixing–dependent phosphorous fluxes in permanently density stratified anoxic natural water. – *Goldschmidt Conference for Geochemistry, Toulouse 1998, Abstract Vol.* 969–970.

MATTIOLI, E. (1997): Nannoplankton productivity and diagenesis in the rhythmically bedded Toarcian–Aalenian Fiuminata section (Umbria–Marche Apennine, central Italy). – *Palaeogeography, Palaeoclimatology, Palaeoecology* 130, 113–133.

McCREA, J. M. (1950): On the isotopic chemistry of carbonates and a paleotemperature scale. – *Journal of Chemical Physics* 18, 849–857

MII, H., GROSSMAN, E. L. & YANCEY, T. E. (1997): Stable carbon and oxygen isotope shifts in Permian seas of West Spitsbergen – Global change or diagenetic artifact? – *Geology* 25/3, 227–230.

MORETTINI, E., BAUMGARTNER, P. O., HUNZIKER, J. C., MONACO, P. & RIPEPE, M. (2000): Stable isotopic signal of carbon and oxygen in Jurassic marlstone–limestone rhythms (Italy, Central Apennines) – *GeoResearh Forum (5th Jurassic Symposium, Vancouver)* 6, 487–498.

MORSE, J. W., MILLERO, F J., CORNWELL, J. C. & RICKARD, D. (1987): The chemistry of the hydrogen sulfide and iron sulfide systems in natural waters. – *Earth Science Reviews* 24, 1–42.

MURRAY, R. W. & LEINEN, M. (1993): Chemical transport to the seafloor of the equatorial Pacific Ocean across a latitudinal transect at 135°W: Tracking sedimentary major, trace, and rare earth element fluxes at the Equator and the Intertropical Convergence Zone. – *Geochimica et Cosmochimica Acta* 57, 4141–4163.

MURRAY, R. W. & LEINEN, M. (1996): Scavenged excess aluminium and its relationship to bulk titanium in biogenic sediment from the central equatorial Pacific Ocean. – *Geochimica et Cosmochimica Acta* 60, 3869–3878.

MURRAY, R. W., BUCHHOLTZ TEN BRINK, M., R., JONES, D. L., GERLACH, D. C. & RUSS, G. P. III (1990): Rare earth elements as indicators of different marine depositional environments in chert and shale. – *Geology* 18, 268–271.

MURRAY, R. W., BUCHHOLTZ TEN BRINK, M., R., JONES, D. L., GERLACH, D. C. & RUSS, G. P. III (1991): Rare earth, major, and trace elements in chert from the Franciscan Complex and Monterey Group, California: assessing REE sources to fine–grained marine sediments. – *Geochimica et Cosmochimica Acta* 55, 1875–1896.

MURRAY, R. W., BUCHHOLTZ TEN BRINK, M., R., GERLACH, D. C., RUSS, G. P., III & JONES, D. L. (1992): Rare earth, major, and trace element composition of Monterey and DSDP chert and associated host sediment: assessing the influence of chemical fractionation during diagenesis. – *Geochimica et Cosmochimica Acta* 56, 2657–2671

MURRAY, R. W., LEINEN, M. & ISEM A. R. (1993): Biogenic flux of Al to sediment in the central equatorial Pcific Ocean. Evidence for increased productivity during glacial periods. – *Paleoceanography* 8, 651–670.

NAGY, E. (1969): Lower Jurassic coal sequence of the Mecsek Mountains. Geology (In Hungarian) – *Annales of the Geological Institute of Hungary* 51/2, 245–971.

NESBITT, H. W. & YOUNG, G. M. (1982): Early Proterozoic climates and plate motions inferred from major elemental chemistry of lutites. – *Nature* 199, 715–717.

NESBITT, H. W., FEDO, C. M. & YOUNG, G. M. (1997): Quartz and feldspar stability, steady and non–steady state weathering, and petrogenesis of siliciclastic sands and. – *Journal of Geology* 105, 173–191.

NORMAN, M. D. & DE DECKKER, P (1990): Trace metals in lacustrine and marine sediments: A case study from the Gulf of Carpentaria, northern Australia. – *Chemical Geology* 82, 299–318.

ODERMATT, J. R. & CURIALE, J. A. (1991): Organically bound metals and biomarkers in the Monterey Formation of the Santa Maria Basin, California. – *Chemical Geology* 91, 99–113.

O'NEIL, J. R., CLAYTON, R. N. & MAYEDA, T. K. (1969): Oxygen isotope fractionation in divalent metal carbonates. – *The Journal of Chemical Physics* 51, 5547–5558.

PACEY, N. R. (1984): Bentonites in the Chalk of central eastern England and their relation to the opening of the northeast Atlantic. – *Earth and Planetary Science Letters*, 67, 48–60.

PANCOST, R. D., FREEMAN, K. H. & PATZKOWSKY, M. E. (1998): Late–Middle Ordovician environmental change: molecular and isotopic evidence from North America. – In: *Goldschmidt Conference for Geochemistry, Toulouse 1998, Abstract Vol.* 1133–1134.

PARHAM, W. E. (1966): Lateral variations of clay mineral assemblages in modern and ancient sediments. – In: GEKKER, K. & Weiss A. (eds.): *Proceedings of International Clay Conferences* 1, 135–145.

PARRISH, J. T., ZIEGLER, A. M. & SCOTESE, C. R. (1982): Rainfall patterns and the distribution of coals and evaporites in the Mesozoic and Cenozoic. – *Palaeogeography, Palaeoclimatology, Palaeoecology* 40, 67–101.

PATTERSON, W. P & WALTER, L. M. (1994): Depletion of ^{13}C in seawater ΣCO_2 on modern carbonate platforms: Significance for the carbon isotopic record of carbonate. – *Geology* 22, 885–888.

PELECHATY, S. M., KAUFMAN, A. J. & GROTZINGER, J. P. (1996): Evaluation of $\delta^{13}C$ chemostratigraphy for intrabasinal correlation: Vendian strata of northeast Siberia. – *Geological Society of America Bulletin* 108, 992–1003.

PINGITORE, N. E., LYTLE, F. W., DAVIES, B. M., EASTMAN, M. P., ELLER, P. G. & LARSON, E. M. (1992): Mode of incorporation of Sr in calcite: determination by X–ray absorption spectroscopy. – *Geochimica et Cosmochimica Acta* 56, 1531–1538.

PIPER, D. Z. (1994): Seawater as the source of minor elements in black shales, phosphorites and other sedimentary rocks. – *Chemical Geology* 114, 95–114.

PITTET, B. & STRASSER, A. (1998): Long–distance correlations by sequence stratigraphy and cyclostratigraphy: examples and implications (Oxfordian from the Swiss Jura, Spain, and Normandy). – *International Journal of Earth Sciences* 86, 852–874.

POPP, B. N., TAKIGIKU, R., HAYES, J. M., LOUDA, J. W & BAKER, E. W. (1989): The post–Paleozoic

chronology and mechanism of ^{13}C depletion in primary marine organic matter. – *American Journal of Science* 289/4, 436–454.

PRATT, L. M. (1984): Influence of paleoenvironmental factors on preservation of organic matter in Middle Cretaceous Greenhorn Formation, Pueblo, Colorado. – *AAPG Bulletin* 68/9, 1146–1159.

PROKOPH, A. & VEIZER, J. (1999): Trends, cycles and nonstationarities in isotope signals of Phanerozoic seawater. – *Chemical Geology* 161, 225–240.

RAISWELL, R. (1987): Non–steady state microbiological diagenesis and the origin of concretions and nodular limestones. – In: MARSHALL, J.D. (ed.): *Diagenesis in Sedimentary Sequences. Geological Society of London Special Publication* 36, 41–54. Blackwell, Oxford.

REYNARD, B. (1998): Partitioning of divalent elements between calcium carbonates and water: A solid solution model and implications for palaeoenvironmental and palaeoecological reconstructions from biogenic carbonates. – In: *Goldschmidt Conference for Geochemistry, Toulouse 1998, Abstract Vol.* 1259–1260.

REYNOLDS, R. C., JR. & HOWER, J. (1970): The nature of interlayering in mixed–layer illite–montmorillonite. – *Clays and Clay Minerals* 18, 25–36.

RICKEN, W (1991): Variation of sedimentation rates in rhythmically bedded sediments: Distinction between depositional types. – In: EINSELE, G., RICKEN, W. & SEILACHER, A. (eds.): *Cycles and Events in Stratification.* Springer, Berlin, Heidelberg, New York, 3–19.

RICKEN, W (1994): Complex rhythmic sedimentation related to third oder sea–level variations: Upper Cretaceous, Westren Interior Basin, USA. – In: DE BOER, P L. & SMITH, D. G. (eds.): *Orbital Forcing and Cyclic Sequences. IAS Special Publications* 19, 167–193.

RICKEN, W. & EDER, W. (1991): Diagenetic modification of calcareous beds – an overview. – In: EINSELE, G., RICKEN, W & SEILACHER, A. (eds.): *Cycles and Events in Stratification.* Springer, Berlin, Heidelberg, New York. 430–449.

RISCHÁK, G. & VICZIÁN, I. (1974): Mineralogical factors determining the intensity of basal reflections of clay minerals. – *Annual Reports of Hungarian Geological Institute* 1972, 229–256. (In Hungarian).

ROBERT, C. & KENNETT, J. P. (1994): Antarctic subtropical humid episode at the Paleocene–Eocene boundary: clay mineral evidence. – *Geology* 22, 211–214.

ROCC Group (Research on Cretaceous Cycles Group) (1986): Rhythmic bedding in Upper Cretaceous pelagic carbonate sequences: varying sedimentary response to climatic forcing. – *Geology* 14, 153–156.

ROBINSON, D. & WRIGHT, V. P. (1987): Ordered illite–smectite and kaolinite–smectite: pedogenic minerals in a Lower Carboniferous paleosol sequence, South Wales. – *Clay Mineralogy* 22, 109–118.

ROSER, B. P & KORSCH, R. J. (1988): Provenance signatures of sandstone–mudstone suites determined using discriminant function analysis of major–element data. – *Chemical Geology* 67, 119–139.

SAVRDA, C. E. & BOTTJER, D. J. (1994): Ichnofossils and ichnofabrics in rhythmically bedded pelagic/hemi–pelagic carbonates: recognition and evaluation of benthic redox and scour cycles. – *Special Publications of International Association of Sedimentologists* 19, 195–210.

SCHMITZ, B. (1987): Barium, equatorial high productivity, and the northward wandering of the Indian continent. – *Paleoceanography* 2, 63–77.

SCHOLLE, P A. (1977): Chalk diagenesis and its relation to petroleum exploration: oil from chalks, a modern miracle? – *AAPG Bulletin* 61, 982–1009.

SCHWARZACHER, W (1975): *Sedimentation Models and Quantitative Stratigraphy. Developments in Sedimentology* 19. – Elsevier, Amsterdam, 382 p.

SETHI, P. S. & LEITHOLD, E. L. (1994): Climatic cyclicity and terrigenous sediment influx to the Early Turonian Greenhorn Sea, Southern Utah. – *Journal of Sedimentary Research* B 64/1, 26–39.

SHAW, T J., GIESKES, J. M. & JAHNKE, R. A. (1990): Early diagenesis in differing depositional environments: The response of transition metals in pore water. – *Geochimica et Cosmochimica Acta* 54, 1233–1246.

SINGER, A. (1984): The paleoclimatic interpretation of clay minerals in sediments – a review. – *Earth Sci. Rev.* 21, 251–293.

ŚRODON, J. (1980): Precise identification of illite/smectite interstratifications by X–ray powder diffraction. – *Clays and Clay Minerals* 28, 401–411.

ŚRODON, J. (1984): X–ray powder diffraction identification of illitic materials. – *Clays and Clay Minerals* 32, 337–349.

SUNDARARAMAN, P., SCHOELL, M., LITTKE, R., BAKER, D. R., LEYTHAEUSER, D. & RULLKÖTTER, J. (1993): Depositional environment of Toarcian shales from northern Germany as monitored with porphyrins. – *Geochimica et Cosmochimica Acta* 57, 4213–4218.

SZABÓ, GY. & BORBÉLY–KISS, I. (1993): PIXYKLM computer package for PIXE analyses. – *Nuclear Instruments and Methods in Physics Research* B75, 123–126.

TAYLOR, S. R. & MCLENNAN, S. M. (1985): *The Continental Crust: Its Composition and Evolution.* Blackwell, Oxford, 312 p.

THUNELL, R., RIO, D., SPROVERI, R. & RAFFI, I. (1991): Limestone–marl couplets: origin of the Early Pliocene Trubi Marls in Calabria, Southern Italy. – *Journal of Sedimentary Petrology* 61/7, 1109–1122.

TÖRÖK, Á (1997a): Dolomitization and karst–related dedolomitization of Muschelkalk carbonates, in South Hungary. – *Acta Geologica Hungarica* 40/4, 441–462.

TÖRÖK, Á (1997b): Triassic ramp evolution in Southern Hungary and its similarities to the Germano–type Triassic. – *Acta Geologica Hungarica* 40/4, 367–390.

TUCKER, M. E. & WRIGHT, V P. (1990): *Carbonate Sedimentology.* – Blackwell Scientific Publications, Oxford, London, 482 p.

VALLADARES, M. I., BARBA, P., UGIDOS, J. M., COLMENERO, J. R. & ARMENTEROS, I. (2000): Upper Neoproterozoic–Lower Cambrian sedimentary successions in the Central Iberian Zone (Spain): sequence stratigraphy, petrology and chemostratigraphy. Implications for other European zones. – *International Journal of Earth Sciences* 89, 2–20.

VANDERAVEROET, P. & DECONINCK, J. F (1997): Clay mineralogy of Cenozoic sediments of the Atlantic City borehole, New Jersey. – *Proceedings of ODP, Scientific Results* 150X, 49–57

VARGA, A., SZAKMÁNY, GY., JÓZSA, S. & MÁTHÉ, Z. (2001): Petrographical and geochemical comparison between the Carboniferous sandstone pebbles of the Lower Miocene conglomerate from Western Mecsek

Mountains and Téseny Sandstone Formation. – *Földtani Közlöny*, in press

VICZIÁN, I. (1987): *Clay Minerals in Sedimentary Rocks of Hungary.* – D.Sc. Thesis, Budapest. p. 205. (In Hungarian).

VICZIÁN, I. (1990): Report of the mineralogical examinations taken on the material of part belongs to the Liassic of the borehole Máza Nb. 26. – Unpublished data in form of manuscript. MÁFI Adattár. Leltári szám 577/32.

VICZIÁN, I. (1994): Smectite–illite geothermometry (In Hungarian with English abstract). – *Földtani Közlöny* 124/3, 367–379.

WATANABE, T. (1981): Identification of illite/montmorillonite interstratifications by X–ray powder diffraction. – *Journal of Mineralogical Society of Japan, Special Issue* 15, 32–41

WEISSERT, H. & BRÉHÉRET, J. G. (1991): A carbonate carbon–isotope record from the Aptian–Albian sediments of the Vocontian trough (SE France). – *Bulletin de Société Géologique de France* 162, 1133–1140.

WEISSERT, H. & MOHR, H. (1996): Late Jurassic and its impact on carbon cycling. – *Palaeogeography, Palaeoclimatology, Palaeoecology* 122, 27–43.

WEISSERT, H., MCKENZIE, J. & HOCHULI, P. (1979): Cyclic anoxic events in the Early Cretaceous Tethys Ocean. – *Geology* 7, 147–151.

WENZEL, B. & JOACHIMSKI, M. M. (1996): Carbon and oxygen isotopic composition of Silurian brachiopods (Gotland/Sweden): palaeoceanographic implications. – *Palaeogeography, Palaeoclimatology, Palaeoecology* 122, 143–166.

YAMAMOTO, K. (1987): Geochemical characteristics and depositional environments of cherts and associated rocks in the Franciscan and Shimanto Terranes. – *Sedimentary Geology* 52, 65–108.

ZHANG, T., KERSHAW, S., WAN, Y & LAN, G. (2000): Geochemical and facies evidence for palaeoenvironmental change during the Late Ordovician Hirnantian glaciation in South Sichuan Province, China. – *Global and Planetary Change* 24/2, 133–152.

ZWOLSMAN, J. J. G., VAN ECK, B. T. M. & VAN DER WEIJDEN, C. H. (1997): Geochemistry of dissolved trace metals (cadmium, copper, zinc) in the Scheldt estuary, southwestern Netherlands: Impact of seasonal variability. – *Geochimica et Cosmochimica Acta* 61, 1635–1652.

Table I. Results of the stable isotopic measurements

number of sample	$\delta^{13}C$ (PDB) values (‰)	$\delta^{18}O$ (PDB) values (‰)
P-24b	2.1	-2.0
P-26b	1.0	-5.1
P-34a	1.9	-2.6
P-34b	2.0	-2.2
P-34c	1.6	-4.4
P-37b	1.2	-4.6
P-38b	2.1	-2.1
P-42a	1.6	-3.0
P-42b	2.0	-2.3
P-43a	0.4	-4.6
P-47	0.2	-4.6
P-48a	1.1	-4.8
K-1a	1.7	-1.4
K-31	1.5	-0.5
K-32	0.8	-2.5
K-48	1.6	-0.5
K-52	1.3	-2.3
K-53	1.0	-4.1
K-54b	1.5	-1.5
K-54c	1.3	-3.2
K-56	1.4	-3.1
K-57	0.7	-4.3
K-58a	1.1	-3.1
K-58b	0.6	-2.8
K-59	0.6	-2.7

Table II. a. Major element concentrations of the examined samples. Data with high standard deviation values are indicated by bold characters

sample	Al_2O_3(%)	SiO_2(%)	CaO(%)	K_2O(%)	TiO_2(%)	MnO(ppm)	Fe_{TOT}(%)
P-24b	3.63±0.7	6.63±0.3	55.25±2.2	0.30±0.03	0.04±0.01	262±30	0.69±0.03
P-26b	5.74±0.8	59.68±2.4	18.33±0.7	1.11±0.50	**0.13±0.06**	188±30	1.08±0.04
P-28d	3.29±0.8	54.97±2.2	22.43±0.9	0.94±0.44	0.15±0.01	194±30	1.03±0.04
P-29a	3.36±0.7	43.10±1 7	27.98±1.1	0.61±0.33	0.13±0.01	247±50	0.85±0.04
P-33	5.63±0.8	51.08±0.5	24.69±1.0	1.07±0.49	0.17±0.01	214±30	1.24±0.05
P-34a	**0.76±0.7**	18.72±0.5	45.50±1.8	0.48±0.03	0.08±0.01	258±30	0.77±0.03
P-34b	3.29±0.7	8.56±0.4	52.27±2.1	0.29±0.03	0.07±0.01	235±30	0.72±0.03
P-34c	5.63±0.7	49.80±1.9	28.06±1.1	0.90±0.04	0.13±0.01	203±30	0.70±0.03
P-36a	37.79±2.0	62.69±2.5	29.02±1.1	0.75±0.04	0.13±0.01	141±20	0.59±0.02
P-37a	12.89±0.9	57.62±2.3	13.64±0.5	2.06±0.08	0.35±0.09	250±40	1.63±0.07
P-37b	5.48±0.9	47.83±1.9	26.06±1.0	1.26±0.06	0.21±0.02	216±30	1.21±0.05
P-38a	**1.10±0.8**	19.94±0.8	46.91±1.9	0.50±0.03	0.09±0.01	217±30	0.68±0.03
P-38b	1.93±0.7	11.89±0.5	50.48±2.0	0.53±0.03	0.10±0.01	239±30	0.69±0.03
P-40a	2.87±0.7	29.15±1.2	38.18±1.5	0.56±0.03	0.11±0.01	178±30	0.84±0.03
P-41	6.61±0.9	49.00±2.0	25.21±1.0	1.39±0.06	0.23±0.02	221±30	1.26±0.05
P-42a	4.61±0.7	16.17±0.7	46.89±1.9	0.42±0.03	0.07±0.01	225±30	0.72±0.03
P-43a	9.64±0.8	53.77±0.8	17.80±0.7	1.70±0.07	0.27±0.02	200±30	1.64±0.07
P-44b	**1.70±0.8**	9.05±0.4	53.43±2.1	0.43±0.03	0.12±0.02	488±50	0.85±0.03
P-45	8.50±0.9	48.11±2.0	24.92±1.0	1.47±0.06	0.26±0.02	234±30	1.33±0.05
P-46b	2.76±0.7	26.59±1.1	42.39±1.7	0.63±0.03	0.11±0.01	214±30	0.81±0.03
P-47	7.71±0.9	57.37±2.3	15.49±0.6	1.97±0.08	0.33±0.02	227±30	1.54±0.06
P-48a	4.27±0.7	47.93±1.9	28.62±1.1	0.77±0.04	0.15±0.01	196±30	0.98±0.04
P-49b	5.06±0.6	45.75±1.9	29.91±1.2	0.82±0.04	0.14±0.01	188±30	0.91±0.04
K-1a	2.42±0.8	13.80±0.6	51.89±2.1	0.30±0.02	**0.03±0.01**	638±50	0.51±0.02
K-22	6.20±0.8	44.17±1.8	29.92±1.2	1.19±0.05	0.16±0.01	296±40	1.06±0.04
K-23	13.79±1.0	57.54±2.3	16.45±0.7	2.36±0.10	0.32±0.02	247±40	1.62±0.07
K-29	6.24±0.8	40.83±1.7	31.62±1.3	1.28±0.06	0.17±0.01	359±40	0.96±0.04
K-32	6.92±0.9	46.84±1.9	21.03±0.8	2.51±0.10	0.30±0.02	258±40	1.70±0.07
K-34	4.35±0.7	40.28±1.6	29.67±1.2	1.57±0.07	0.21±0.02	332±40	1.16±0.05
K-35	4.27±0.8	47.55±1.9	22.47±0.9	2.32±0.10	0.28±0.02	235±40	1.53±0.06
K-36	**1.36±0.8**	23.57±1.0	43.33±1.7	0.66±0.04	0.08±0.01	318±40	0.85±0.04
K-44	3.78±0.7	37.05±1.5	29.39±1.2	1.85±0.08	0.23±0.02	376±40	1.34±0.05
K-45	8.05±0.7	38.91±1.6	27.67±1.1	2.10±0.90	0.27±0.02	341±40	1.39±0.06
K-48	4.16±0.7	9.15±0.4	49.65±2.0	0.33±0.03	**0.03±0.01**	385±40	0.40±0.01
K-52	4.16±0.9	11.74±0.5	51.65±2.1	0.36±0.03	0.04±0.01	542±40	0.59±0.02
K-53	9.11±0.9	45.73±1.9	22.66±0.9	2.37±0.10	0.30±0.02	372±40	1.64±0.07
K-54b	**0.76±0.8**	27.57±1.1	41.75±1.7	0.68±0.04	0.06±0.01	528±50	0.66±0.03
K-54c	5.18±0.8	23.14±1.0	43.15±1.7	0.55±0.03	0.06±0.01	580±50	0.77±0.03
K-56	5.03±0.8	31.25±1.3	37.02±1.5	0.80±0.04	0.11±0.01	452±40	0.69±0.03

Table II. b.　Major element concentrations of the examined samples. Data with high standard deviation values are indicated by bold characters

K-57	11.79±0.8	43.59±1.8	23.53±0.9	2.67±0.11	0.32±0.02	381±40	1.60±0.07
K-58a	**1.02±0.9**	33.20±1.4	38.58±1.6	0.97±0.05	0.12±0.01	553±40	0.85±0.03
K-58b	6.20±0.8	40.21±1.6	29.63±1.2	1.43±0.06	0.19±0.02	520±50	1.58±0.06
K-59	12.40±0.9	47.10±1.9	20.45±0.8	3.43±0.14	0.41±0.02	435±40	2.02±0.08
K-60	3.67±0.9	28.92±1.2	40.33±1.6	0.96±0.05	0.13±0.01	600±50	0.89±0.04
K-61	11.71±0.9	40.71±1.7	27.06±1.1	2.41±0.10	0.27±0.02	524±50	1.50±0.06
ave-rage 1	5.06±0.8	29.58±1.2	39.20±1.6	0.80±0.04	0.11±0.02	347±40	0.85±0.03
ave-rage 2	7.94±0.8	48.47±1.9	23.24±0.9	1.75±0.08	0.26±0.02	288±40	1.42±0.05

Table III. a. Trace element concentrations of the examined samples. Data with high standard deviation values are indicated by bold characters

sample	Rb (ppm)	Sr (ppm)	V (ppm)	P (ppm)	Ni (ppm)	Cu (ppm)	Zn
P-24b	-	735±50	-	6303±410	-	-	14±6
P-26b	44±13	424±40	-	-	-	22±6	43±6
P-28d	45±17	500±50	-	-	-	20±7	36±7
P-29a	35±16	589±50	-	1966±520	-	-	27±1
P-33	**26±13**	468±40	-	**1012±550**	-	17±6	53±7
P-34a	31±14	721±50	-	5924±410	-	11±5	50±7
P-34b	40±15	862±50	-	5593±370	-	14±5	22±6
P-34c	29±13	464±40	98±45	3323±600	-	16±6	35±6
P-36a	**19±12**	449±40	**76±43**	3584±650	-	23±6	30±6
P-37a	47±13	190±30	-	1730±640	**31±16**	30±7	55±8
P-37b	36±14	420±40	104±54	2705±590	-	20±6	50±7
P-38a	44±14	692±50	-	5452±490	-	**12±6**	24±6
P-38b	37±14	700±50	-	6618±440	-	15±6	28±6
P-40a	41±14	563±40	-	3464±480	-	16±6	34±6
P-41	41±14	390±40	144±55	1750±570	-	17±6	51±8
P-42a	54±15	742±50	**90±53**	5126±420	-	**12±6**	21±6
P-43a	41±13	308±30	-	2278±580	**24±16**	24±6	67±8
P-44b	43±14	724±50	-	8739±550	**20±12**	14±6	24±6
P-45	40±13	335±30	-	2169±560	-	22±7	54±8
P-46b	43±12	586±40	-	4788±500	-	11±5	28±6
P-47	51±13	247±30	157±56	-	-	16±6	68±8
P-48a	40±14	534±40	137±45	2103±560	-	21±6	29±6
P-49b	35±14	471±40	-	2927±560	-	20±6	44±7
K-1a	25±11	377±30	-	8027±500	-	**11±6**	15±5
K-22	46±15	420±40	-	1914±540	-	20±7	46±8
K-23	52±15	225±30	121±53	-	**26±16**	23±7	62±8
K-29	52±14	376±40	-	2723±550	**24±13**	19±7	42±7
K-32	56±15	261±30	131±59	-	-	25±7	75±9
K-34	41±15	368±40	-	2762±530	**29±15**	19±7	52±8
K-35	38±14	259±30	-	2144±580	**28±16**	21±7	69±9
K-36	44±15	534±40	-	5404±490	**22±12**	15±6	37±7
K-44	55±15	284±30	**107±57**	3123±500	31±15	25±7	58±8
K-45	57±16	269±30	**107±59**	1883±510	31±15	23±7	68±8
K-48	**22±13**	488±40	-	7083±430	-	**10±6**	14±6
K-52	**19±13**	491±40	-	6880±460	-	14±6	20±6

Table III. b. Trace element concentrations of the examined samples. Data with high standard deviation values are indicated by bold characters

K-53	56±15	263±30	176±60	1334±600	**30±16**	16±7	87±9
K-54b	40±12	378±30	-	6536±520	-	-	17±6
K-54c	28±13	447±40	-	6919±490	**19±11**	**10±6**	33±6
K-56	**25±12**	383±30	84±41	5025±490	**20±11**	14±5	27±6
K-57	58±15	281±30	141±60	3877±540	32±16	25±7	83±9
K-58a	34±12	397±30	-	5720±560	23±11	13±6	29±6
K-58b	37±13	306±30	**102±55**	4722±550	**26±15**	15±6	53±7
K-59	54±15	197±30	137±67	3363±550	41±18	26±7	102±10
K-60	36±12	373±30	-	5984±530	**19±12**	**12±6**	35±6
K-61	54±15	277±30	-	4904±540	32±15	21±7	62±8
average 1	36±13	508±40	102±50	5150±500	**24±13**	15±6	32±6
average 2	45±14	321±30	137±60	2428±560	**31±16**	21±7	63±8

Table IV Correlation matrix calculated from the measured concentrations

	Al	Si	P	K	Ca	Ti	**V**	Mn	Fe	Ni	Cu	Zn	Rb	Sr
Al	1	0.544	-0.326	0.384	-0.449	0.414	-0.233	-0.213	0.290	0.615	0.523	0.332	0.009	-0.383
Si		1	-0.851	0.625	-0.959	0.700	0.301	-0.397	0.645	0.587	0.734	0.617	0.269	-0.670
P			1	-0.567	0.870	-0.679	-0.659	0.552	-0.623	-0.619	-0.695	-0.616	-0.344	0.470
K				1	-0.773	0.956	0.610	0.024	0.935	0.912	0.725	0.940	0.664	-0.809
Ca					1	-0.835	-0.654	0.338	-0.801	-0.686	-0.786	-0.761	-0.433	0.751
Ti						1	0.707	-0.144	0.952	0.870	0.769	0.920	0.652	-0.755
V							1	0.061	0.676	0.512	0.103	0.685	0.599	-0.473
Mn								1	-0.076	-0.314	-0.332	-0.082	-0.113	-0.256
Fe									1	0.830	0.709	0.932	0.628	-0.725
Ni										1	0.772	0.871	0.725	-0.694
Cu											1	0.654	0.494	-0.608
Zn												1	0.614	-0.708
Rb													1	-0.325
Sr														1

Table V Ti–normalised enrichment factors relative to the PAAS values (TAYLOR & MCLENNAN 1985). Data of samples from carbonate–rich semicouplets are indicated by bold characters. LOQ: under the limit of quantification

sample	SiO_2	Al_2O_3	Fe_{TOT}	MnO	CaO	K_2O	P	Rb	Sr	V	Ni	Cu	Zn
P-24B	**2.6**	**4.8**	**2.7**	**6.0**	**1062.5**	**2.0**	**98.5**	**LOQ**	**92.0**	**LOQ**	**LOQ**	**LOQ**	**3.9**
P-26B	**7.3**	**2.3**	**1.3**	**1.3**	**108.5**	**2.3**	**LOQ**	**2.1**	**16.5**	**LOQ**	**LOQ**	**3.4**	**3.7**
P-28D	5.8	1.2	1.1	1.2	115.	1.7	LOQ	1.9	16.5	LOQ	LOQ	2.6	2.7
P-29A	**5.3**	**1.4**	**1.0**	**1.7**	**165.6**	**1.3**	**9.4**	**1.7**	**22.5**	**LOQ**	**LOQ**	**LOQ**	**2.3**
P-33	4.8	1.8	1.1	1.2	111.7	1.7	3.8	0.9	14.0	LOQ	LOQ	2.0	3.4
P-34A	**3.7**	**0.5**	**1.5**	**2.9**	**437.5**	**1.6**	**46.3**	**2.4**	**45.0**	**LOQ**	**LOQ**	**2.8**	**7.0**
P-34B	**2.0**	**2.5**	**1.6**	**3.1**	**574.4**	**1.1**	**49.9**	**3.3**	**61.5**	**LOQ**	**LOQ**	**4.0**	**3.4**
P-34C	**6.1**	**2.3**	**0.8**	**1.5**	**166.0**	**1.9**	**16.0**	**1.4**	**18.0**	**5.0**	**LOQ**	**2.4**	**3.0**
P-36A	**7.7**	**15.4**	**0.7**	**1.0**	**171.7**	**1.6**	**17.3**	**0.9**	**17.5**	**3.9**	**LOQ**	**3.6**	**2.6**
P-37A	2.6	2.0	0.7	0.6	30.0	1.6	3.1	0.8	2.5	LOQ	1.5	1.8	1.8
P-37B	3.6	1.4	0.9	0.9	95.5	1.6	8.1	1.1	10.0	3.3	LOQ	2.0	2.7
P-38A	**3.5**	**0.7**	**1.2**	**2.2**	**400.9**	**1.5**	**37.9**	**3.1**	**38.5**	**LOQ**	**LOQ**	**2.6**	**3.0**
P-38B	**1.9**	**1.0**	**1.1**	**2.2**	**388.3**	**1.4**	**41.4**	**2.3**	**35.0**	**LOQ**	**LOQ**	**3.0**	**3.1**
P-40A	**4.2**	**1.4**	**1.2**	**1.5**	**267.0**	**1.4**	**19.7**	**2.3**	**25.5**	**LOQ**	**LOQ**	**3.0**	**3.4**
P-41	3.4	1.5	0.8	0.9	84.3	1.6	4.8	1.1	8.5	4.2	LOQ	1.4	2.4
P-42A	**3.7**	**3.5**	**1.6**	**2.9**	**515.3**	**1.6**	**45.8**	**4.8**	**53.0**	**8.6**	**LOQ**	**3.4**	**3.3**
P-43A	3.2	1.9	0.9	0.6	50.7	1.7	5.3	0.9	5.5	LOQ	1.5	1.8	2.8
P-44B	**1.2**	**0.8**	**1.1**	**3.7**	**342.5**	**1.0**	**45.5**	**2.3**	**30.0**	**LOQ**	**2.8**	**2.4**	**2.2**
P-45	3.0	1.7	0.8	0.8	73.7	1.5	5.2	0.9	6.5	LOQ	LOQ	1.6	2.3
P-46B	**3.9**	**1.3**	**1.1**	**1.7**	**296.4**	**1.6**	**27.2**	**2.4**	**26.5**	**LOQ**	**LOQ**	**2.0**	**2.8**
P-47	2.8	1.2	0.7	0.6	36.1	1.6	LOQ	0.9	3.5	3.2	LOQ	1.0	2.3
P-48A	**5.1**	**1.5**	**1.0**	**1.2**	**146.8**	**1.4**	**8.8**	**1.7**	**18.0**	**6.1**	**LOQ**	**2.8**	**2.1**
P-49B	5.2	1.9	1.0	1.2	164.3	1.6	13.1	1.6	17.0	LOQ	LOQ	2.8	3.4
K-1A	**7.3**	**4.3**	**2.6**	**19.4**	**1330.5**	**2.7**	**167.3**	**5.2**	**63.0**	**LOQ**	**LOQ**	**7.4**	**5.6**
K-22	4.4	2.1	1.0	1.7	143.9	2.0	7.5	1.8	13.0	LOQ	LOQ	2.6	3.2
K-23	**2.9**	**2.3**	**0.8**	**0.7**	**39.6**	**2.0**	**LOQ**	**1.0**	**3.5**	**2.5**	**1.3**	**1.4**	**2.1**
K-29	**3.8**	**1.9**	**0.9**	**1.9**	**143.1**	**2.0**	**10.0**	**1.9**	**11.0**	**LOQ**	**2.3**	**2.2**	**2.8**
K-32	2.5	1.2	0.9	0.8	53.9	2.3	LOQ	1.2	4.5	2.9	LOQ	1.6	2.8
K-34	**3.1**	**1.1**	**0.9**	**1.5**	**108.7**	**2.0**	**8.3**	**1.3**	**9.0**	**LOQ**	**2.3**	**1.8**	**2.8**
K-35	2.7	0.8	0.8	0.7	61.7	2.2	4.8	0.9	4.5	LOQ	1.7	1.6	2.8
K-36	**4.7**	**0.9**	**1.6**	**3.6**	**416.6**	**2.2**	**42.3**	**3.4**	**33.5**	**LOQ**	**4.7**	**3.8**	**5.1**
K-44	**2.6**	**0.9**	**0.9**	**1.5**	**98.3**	**2.2**	**8.5**	**1.5**	**6.0**	**3.1**	**2.2**	**2.2**	**2.8**
K-45	2.3	1.6	0.8	1.2	78.8	2.1	4.4	1.3	5.0	2.7	1.8	1.8	2.8
K-48	**4.9**	**7.3**	**2.0**	**11.6**	**1273.1**	**3.0**	**147.6**	**4.6**	**81.5**	**LOQ**	**LOQ**	**6.6**	**5.2**
K-52	**4.7**	**5.5**	**2.3**	**12.4**	**993.3**	**2.4**	**107.5**	**0.2**	**61.5**	**LOQ**	**LOQ**	**7.0**	**5.6**
K-53	2.4	1.6	0.8	1.1	58.1	2.1	2.8	1.2	4.5	3.9	1.7	1.0	3.2
K-54B	**7.3**	**0.7**	**1.7**	**8.0**	**535.3**	**3.0**	**68.1**	**4.2**	**31.5**	**LOQ**	**LOQ**	**LOQ**	**3.1**
K-54C	**6.1**	**4.6**	**2.0**	**8.8**	**553.2**	**3.1**	**72.1**	**2.9**	**37.5**	**LOQ**	**5.3**	**3.4**	**6.1**
K-56	**4.5**	**2.4**	**1.0**	**3.7**	**258.9**	**2.0**	**28.6**	**1.4**	**17.5**	**5.1**	**3.0**	**2.6**	**2.8**
K-57	2.2	2.0	0.8	1.1	56.6	2.3	7.6	1.1	4.5	2.9	1.7	1.6	2.9
K-58A	**4.4**	**0.5**	**1.1**	**4.2**	**247.3**	**2.2**	**29.8**	**1.8**	**16.5**	**LOQ**	**3.2**	**2.2**	**2.7**
K-58B	**3.4**	**1.7**	**1.3**	**2.5**	**120.0**	**2.0**	**15.6**	**1.2**	**8.0**	**3.6**	**2.3**	**1.6**	**3.1**
K-59	1.8	1.6	0.8	1.0	38.4	2.3	5.1	0.8	2.5	2.2	1.7	1.2	2.8
K-60	**3.5**	**1.5**	**1.1**	**4.2**	**238.6**	**2.0**	**28.8**	**1.8**	**14.5**	**LOQ**	**2.5**	**1.8**	**3.0**
K-61	2.4	2.3	0.9	1.7	77.1	2.4	11.4	1.3	5.0	LOQ	2.0	1.6	2.6